NASA CR- 72116

NOLTR 66-202

GPO PRICE $ _____

CFSTI PRICE(S) $ _____

Hard copy (HC) 2.00

Microfiche (MF) .65

ff 653 July 65

OPACITY OF HOT, HIGHLY COMPRESSED HYDROGEN

by

G. T. Lalos and G. L. Hammond

prepared for

NATIONAL AERONAUTICS AND SPACE ADMINISTRATION

Interagency Number C-80708

FACILITY FORM 602

N67-27303 (ACCESSION NUMBER)

(THRU)

52 (PAGES)

1 (CODE)

NASA CR-72116 (NASA CR OR TMX OR AD NUMBER)

25 (CATEGORY)

U.S. NAVAL ORDNANCE LABORATORY

NOTICE

This report was prepared as an account of Government sponsored work. Neither the United States, nor the National Aeronautics and Space Administration (NASA), nor any person acting on behalf of NASA:

A.) Makes any warranty or representation, expressed or implied, with respect to the accuracy, completeness or usefulness of the information contained in this report, or that the use of any information, apparatus, method, or process disclosed in this report may not infringe privately owned rights; or

B.) Assumes any liabilities with respect to the use of, or for damages resulting from the use of any information, apparatus, method or process disclosed in this report.

As used above, "person acting on behalf of NASA" includes any employee or contractor of NASA, or employee of such contractor, to the extent that such employee or contractor of NASA, or employee of such contractor prepares, disseminates, or provides access to, any information pursuant to his employment or contract with NASA, or his employment with such contractor.

Requests for copies of this report should be referred to

National Aeronautics and Space Administration
Office of Scientific and Technical Information
Attention: AFSS-A
Washington, D. C. 20546

NASA CR - 72116
NOLTR 66-202

FINAL REPORT

OPACITY OF HOT, HIGHLY COMPRESSED HYDROGEN

by

G.T. Lalos and G.L. Hammond

prepared for

NATIONAL AERONAUTICS AND SPACE ADMINISTRATION

November 16, 1966

Interagency Number C-80708

Technical Management
NASA Lewis Research Center
Cleveland, Ohio
Nuclear Systems Division
R.W. Patch

NAVAL ORDNANCE LABORATORY
White Oak, Maryland

ABSTRACT

The rapid gas compression technique employing a ballistic piston compressor was adapted to the study of the opacity of hydrogen at elevated pressures and temperatures. Hydrogen/helium mixtures were compressed for short times to pressures and temperatures exceeding 2500 atmospheres and 5000°K, and the emission spectra were recorded and analyzed. The discrete line spectra were identified as due to metallic impurities, but the strong background continua could not be ascribed unequivocally to hydrogen. Computer calculations of the specie concentrations that comprise hot, highly compressed hydrogen/helium mixtures were made, and possible opacity producing mechanisms were advanced to explain the observed continua.

TABLE OF CONTENTS

Section		Page
	ABSTRACT	i
	LIST OF ILLUSTRATIONS	iii
1.0	INTRODUCTION	1
2.0	BALLISTIC PISTON COMPRESSOR EXPERIMENTS	2
	2.1 Basic Technique	2
	2.2 Equilibrium Concentrations	5
	2.3 Experimental Techniques	7
	2.3.1 Gas Sample Production	7
	2.3.2 Emission Experiments	10
	2.3.3 Absorption Experiments	12
3.0	EXPERIMENTAL RESULTS	14
	3.1 Pure Hydrogen Experiments	14
	3.2 Hydrogen/Helium Mixture Experiments	15
	3.2.1 Emission Experiments with Mixtures	16
	3.2.2 Absorption Experiments with Mixtures	18
4.0	DISCUSSION AND CONCLUSIONS	21
	REFERENCES	25
	FIGURES	27

LIST OF ILLUSTRATIONS

Figure		Page
1	Ballistic Piston Compressor	27
2	Ballistic Piston Compressor (Reservoir End)	28
3	Ballistic Piston Compressor (High Pressure End)	29
4	Details of Side Window Test Section	30
5	Oscilloscope Record of Test Gas Pressure versus Time	31
6	Temperature versus Neutral Particle Density	32
7	Particle Density versus Pressure for Pure H_2 . . .	33
8	Particle Density versus Mixture Ratio for P = 3000 Atmospheres	34
9	Particle Density versus Pressure for 10/90 H_2/He Mixture Ratio	35
10	Piston with Seals and High Temperature Resistant Head	36
11	Telescopic Minimum Separation Gage	37
12	Optics for Emission Experiments	38
13	Optics for Absorption Experiments	39
14	Time Resolved Spectra for Pure Helium and for 10% Hydrogen Mixture at 6000°K	40
15	Densitometer Tracings of the 10/90 H_2/He Mixture Ratio Spectrogram	41
16	Continua Intensities versus Wavelength	46
17	Oscilloscope Records for Line Opacity Measurements	47
18	Oscilloscope Records for Continuum Opacity Measurements	48

1.0 INTRODUCTION

An order of magnitude increase in specific impulse is required for future space missions. One advanced concept for achieving this is the gaseous core nuclear rocket engine using fissioning uranium plasma as the energy source and hydrogen gas as the propellant. The transparency of hydrogen to radiation from the core constitutes a critical design problem. The ability to impart opacity to the hydrogen is necessary both from the standpoint of keeping radiative heat transfer to the engine walls to a minimum, and for further heating of the hydrogen gas before it exits the nozzle. Temperatures upward of 5000°K are generally regarded as necessary to produce sufficient concentrations of H, H^-, and free electrons to result in useful levels of opacity. An additional operating requirement is a working pressure of as much as 1000 atmospheres to insure core criticality. This high working pressure results in high particle densities and consequently in an increase in opacity.

Conventional methods of experimentally determining gas opacities, i.e., methods employing furnaces, flames, and arcs (high temperatures, low pressures) and static gas compression (low temperature, high pressure) are inadequate for making the required measurements. Recourse must be made to a rapid gas compression technique that produces simultaneous values of gas temperature and pressure of over 5000°K and 1000 atmospheres (Reference 1). This technique, currently being employed in spectral line shape studies (References 2, and 3), utilizes a free, tight-fitting piston in a closed-end tube as the gas container. Firing the free piston toward the end-plug compresses the trapped gas momentarily and allows high gas pressures and temperatures to be attained for times of about

½ millisecond. The high pressures and temperatures persist long enough to permit measurements of the physical state of the gas to be made, but are not of sufficient duration to result in severe damage to the apparatus. By suitably choosing the experimental parameters the rapidity of the compression process can be made sufficiently high to result in an essentially adiabatic compression of the gas while not exceeding the compression rate that produces shock waves.

This report describes the adaption of the rapid gas compression technique to the study of gas opacities at high pressures and temperatures. The approach was to increase the peak pressures and temperatures of pure hydrogen and hydrogen/helium mixtures progressively in the ballistic piston compressor until measureable hydrogen opacity was attained.

2.0 BALLISTIC PISTON COMPRESSOR EXPERIMENTS

2.1 Basic Technique

The Ballistic Piston Compressor used in this investigation is shown in Figure 1. It consists of a high pressure gas reservoir containing the piston driver gas, a piston release section, a 5 centimeter bore diameter tube 4 meters long, and a high pressure section. The basic apparatus is designed for a maximum pressure of 10,000 atmospheres. A cross-sectional view of the reservoir and piston release section is shown in Figure 2, and of the high pressure section in Figure 3. The radiation viewing window in this figure can be replaced with a piezoelectric pressure gage for pressure-time measurements. A cross-sectional view (end-on) of a high pressure section designed with diametrically opposite windows for studies requiring attenuation of a test beam as in the present studies is shown in Figure 4. When this high pressure section is

used, a pressure gage is installed in the end-plug making it possible to make pressure-time and test beam attenuation-time measurements simultaneously. Both the test section shown in Figure 3 and the one containing side windows have chromium plated bores to suppress vaporization of the steel walls by the hot test gas. The compressor is mounted on ball bearings so that its recoil motion is not transmitted to the tables.

To operate the compressor, high pressure gas is admitted behind the plunger (see Figure 2), moving it to the forward position. In this position the reservoir is sealed off from the tube by the forward o-ring on the plunger. The next step involves charging the tube with the gas to be studied and the reservoir with driver gas. Normally the gas used to drive the piston is the same as the test gas under investigation. In this way any gas leakage across the piston does not contaminate the test gas sample. This procedure was modified for the present studies and is discussed in section 2.3.1. The initial pressure of the test gas and the reservoir pressure are chosen to give the desired peak conditions in the test gas. Typically a reservoir pressure of 37 atmospheres driving the piston into a monatomic test gas at one atmosphere initial pressure will generate a maximum test gas pressure of 2000 atmospheres. After the first compression stroke the free piston rebounds and then produces additional lower pressure compressions of the test gas until friction with the compressor walls brings the piston to rest with approximately equal test gas and reservoir gas pressures.

The dynamic nature of the gas compression produced by the free piston is shown in Figure 5. Figure 5(a) is an oscilloscope record of the pressure of the test gas versus time with a sweep speed sufficiently slow to show the complete history from the time of piston release to the time the piston comes to its final rest position. All measurements are made during the period of maximum pressure of the first compression cycle. In Figure 5(b) the scope

sweep speed was increased to show the pressure profile of the first two compression strokes in more detail. Pressure pulse half-widths are typically a few milliseconds and can range from $\frac{1}{2}$ to 10 milliseconds by proper selection of piston mass and reservoir pressure. A further increase in scope sweep speed was made in Figure 5(c). The multiple traces on this record show the pressure-time history of the first compression cycle. A voltage pulse indicating the opening of a spectrograph slit by a high-speed electromechanical shutter can also be seen. This shutter is used in emission studies to allow gas radiation to enter the spectrograph only during the time interval during which the gas pressure is greater than 90% of its peak value. These times are typically 300 microseconds long.

A comparison of the ranges of temperature and density that can be produced by the ballistic piston compressor and by the more conventional static compression and shock tube techniques is shown in Figure 6. Although the ballistic piston compressor and the shock tube both rely on rapid gas compression to overcome the limitations imposed by the melting point of the container the former is characterized by high neutral particle densities, whereas the latter is generally used where high charged particle densities are important.

The isentrope that a gas follows when compressed in the ballistic piston compressor is determined by its initial pressure and temperature. Isentropes corresponding to initial gas pressures of $\frac{1}{2}$, 1 and 2 atmospheres and an initial temperature of 298°K are shown. Low initial pressures produce conditions approaching those generated by the shock tube, whereas high initial pressures result in conditions approaching those generated by static compression. Intermediate initial gas pressures such as the 1 atmosphere value used in this study will produce quite respectable values of neutral and charged particle density simultaneously. The computer program described in the next section was written to facilitate the computation of the number density of the various species that comprise gases and gas mixtures at elevated pressures and temperatures.

2.2 Equilibrium Concentrations

A computational technique for determining chemical equilibrium in complex mixtures of neutral chemical species (Reference 4) was extended to include systems involving charged particles (Reference 5). This method is based on the minimization of the Gibbs free energy function as opposed to the older methods which require knowledge of equilibrium constants and which expressed the abundance of certain chosen species in terms of the abundances of other arbitrarily chosen species. The present method is applicable to all equilibrium reactions and makes possible the computation of equilibrium concentrations of neutral and charged product species of complex gas mixtures with relative ease. The basic computational scheme calculates equilibrium concentrations for any given pressure and temperature. A variation of this permits the calculation to be made as a function of pressure and energy added to the system in the form of a chemical reaction or mechanical work performed by a piston compressing a gas. A second variation consists of calculating equilibrium along an isentrope. The basic scheme (vs P and T) and the first variation (vs P and ΔE) have been programmed in Fortran IV. The computer program has been named PLASMA.

Rapid compression of hydrogen gas along the NTP isentrope to progressively higher pressures will ultimately result in sufficient concentrations of dissociated and ionized species to produce opacity. Because of the low ratio of specific heats of a diatomic gas, i.e., γ of 1.4, very high pressures must be reached before the temperature becomes sufficiently high to produce appreciable dissociation or ionization of the gas. PLASMA program calculations of specie concentration versus total gas pressure were made and are shown in Figure 7. The temperatures used in these calculations are those of an ideal non-dissociating gas. Although admittedly an approximation, it should be sufficiently accurate in view of the low fractional dissociation involved. A pressure of 3,000 atmospheres results in

a H_2 concentration of $7.38 \times 10^{21} cm^{-3}$ and a H concentration of $1.74 \times 10^{19} cm^{-3}$. The free electron concentration is less than $10^{14} cm^{-3}$.

An additional shortcoming of using a pure diatomic gas ($\gamma = 1.40$) as opposed to a monatomic gas ($\gamma = 1.67$) is the much smaller minimum volumes that accompany a given pressure ratio. This effect will ultimately interfere with any measurement involving attenuation of a test beam because of the blocking of the test beam by the piston. The first problem (low temperature) is solved and the second problem (low volume) is alleviated by using hydrogen/helium mixtures. Figure 8 gives the PLASMA program specie concentration results as a function of hydrogen/helium mixture ratio for a total gas pressure of 3000 atmospheres. This plot was used to determine the mixture ratio that optimized the concentration of atomic hydrogen. A 20/80 hydrogen/helium mixture ratio is seen to result in the optimum atomic hydrogen concentration, namely $3.5 \times 10^{20} cm^{-3}$. This represents a twenty-fold increase over the pure hydrogen case for the same maximum pressure. The He, H_2, and free electron concentrations are $2.9 \times 10^{21} cm^{-3}$, $5.4 \times 10^{20} cm^{-3}$, and $6.5 \times 10^{14} cm^{-3}$, respectively. Some of the experiments described in sections 2.3.2 and 2.3.3 were made using this mixture ratio. A 10/90 hydrogen/helium mixture ratio was also used. This gives an increase in calculated temperature of about 700°C and results in approximately the same atomic hydrogen and helium concentrations as in the 20/80 mixture ratio, but with a decrease in H_2 concentration to $1.6 \times 10^{20} cm^{-3}$, and an increase in free electron concentration to $2.8 \times 10^{15} cm^{-3}$.

Examination of the computer results of particle density versus mixture ratio for pressures from 1000 atmospheres to 5000 atmospheres (plotted as in Figure 8) revealed a very weak dependence on pressure (and temperature) of the value of the mixture ratio for optimum atomic hydrogen concentration. The non-dissociating gas approximation in the calculation of the temperature mentioned earlier thus

does not have a significant effect on the choice of mixture ratio. Although a more accurate temperature calculation could have been made the approximation used gives specie concentrations that are within the accuracy required for the present investigation.

Figure 9 shows N_i plotted versus total gas pressure for a 10/90 mixture ratio. Above 1000 atmospheres the H_2 and He particle densities are relatively insensitive to pressure, whereas the H and especially the free electron densities have an appreciable pressure dependence. The cross-over point, i.e., equal densities of two species, occurs at 2000 atmospheres for H_2 and H.

2.3 Experimental Techniques

2.3.1 Gas Sample Production

The experimental investigations of this report were made by compressing pure hydrogen, 20/80 and 10/90 hydrogen/helium mixtures, and pure helium in the ballistic piston compressor assembled with the side-window high pressure section with chromium-plated bore. The initial test gas conditions were 1 atmosphere pressure and room temperature, 298°K. Sixty compressor shots were made at pressures up to 3170 atmospheres. Of these approximately 40 were made to check out the opacity measuring optics and to evaluate various operating parameters, while the remaining 20 were made to record emission and absorption spectra.

The regular procedure of using the same gas as test gas and piston driver gas was discarded in these experiments for safety as well as economy purposes. A large reservoir filled with high pressure hydrogen would constitute an unnecessary safety hazard in the mixture shots, whereas dumping all the reservoir gas each time the test gas mixture ratio was changed would be an unnecessary expense. Commercial helium of 99.99% purity was used as the driver gas in all

of the experiments. In addition, two independent gas flow systems were constructed for evacuating, flushing, and filling the compressor with driver gas and with test gas. This was done in order to eliminate any possibility of error in the composition of the test gas due to leaky valves or to operator error. The flow system for the test gas was supplied with either commercial helium or commercial hydrogen of 99.9% purity, and the system was capable of filling the test section with a mixture of these two gases to an estimated accuracy of 1% in the mixture ratio.

Cleaning procedures were employed before each shot, and precautions were taken to prevent undue contamination of the test gases. The bore of the steel tube and the chromium plated test section were cleaned by drawing acetone soaked swabs through them. Other solvents occasionally used included water and methanol. Brass and bronze ablation deposits were removed by soaking the test section bore in warm chromic acid for about twelve hours. Filters which remove particles larger than 25 microns were installed at all supply tank outlets and at all gas inlet ports in the compressor.

In order to prevent reservoir gas from leaking across the piston during the compression stroke and altering the test gas mixture ratio, a cup-type Teflon piston seal was designed and installed on the rear-end of the piston. Assembly is made with the open end of the cup seal facing the reservoir. When the reservoir gas impinges on the rear of the piston the Teflon cup is forced to expand radially reducing the clearance with the tube bore to zero and producing an effective gas seal. This step accomplished its purpose but of course resulted in a test gas sample at the end of the compression stroke deprived of any gain in mass from the reservoir gas, but still vulnerable to gas leakage across the piston and Teflon seal and into the reservoir during the high pressure part of the compression cycle. Visual inspection of the walls of the high pressure section immediately after a low-temperature compressor shot revealed dust

patterns that suggested abnormally small minimum separations between the end-plug and piston. On high-temperature shots small deposits of brass ablated from the side window jackets were found on the side walls of the forward part of the piston, again indicating smaller minimum separations than expected. These observations were followed by placing a second cup-type Teflon seal on the piston just forward of the rear seal. In this case the open side of the seal faces the test gas and its sealing action is actuated as the test gas pressure begins to grow. Figure 10 shows the phosphor-bronze piston body assembled with the two cup seals and with the solid molybdenum, high-temperature resistant piston head. The outer diameter of all the components of the piston are undercut a few mils from the 1.968 inch diameter of the four parts of the piston body that bear on the 1.972 inch diameter tube walls. The diameter of the bearing surfaces of the Teflon seals is made approximately equal to the bore diameter of the tube. Results of tests with both seals installed showed that the forward seal functioned properly and increased the minimum piston/end-plug separation over the value obtained with the single rear seal. Although the performance of the piston seals appears satisfactory, some seal failures did occur on compressor shots with peak pressures over 2000 atmospheres. Some further developmental work on the seals seems desirable.

Accurate information on the minimum piston/end-plug separation is necessary in shots involving the attenuation of a test beam by the test gas. A decrease in test beam signal strength due to the partial blockage of the test beam by the piston at the end of the compression stroke can easily be interpreted as a sign of gas opacity. In order to guard against this happening, a telescopic minimum separation gage was designed and constructed. When in use it is installed in the end-plug in place of the pressure gage as shown in Figure 11. It consists of two concentric interference-fit tubes, the outer one imbedded in a steel plug which is mounted flush with the face of the end-plug. The inner tube is slotted

along its length and is free to move into the outer tube when sufficient force is applied, i.e., by the piston at the end of the first compression stroke. The interference fit is adjusted so that the force necessary to produce relative motion between the two tubes is not sufficient to affect the ballistics of the piston, nor so loose that the inner tube continues its motion relative to the outer tube after the piston has reversed directions at the end of the compression stroke. As shown in Figure 11 three pairs of tubes of the lengths indicated give a useful measuring range of 46.25 millimeters down to 5.00 millimeters. A calibration of the compressor consists of measuring the minimum piston/end-plug separation as a function of pressure for a given gas mixture and piston configuration. The telescopic gage is used only for obtaining the piston/end-plug calibration. It is removed and replaced by the pressure gage when emission or absorption studies are being made.

2.3.2 Emission Experiments

Emission spectrography of pure H_2, H_2/He mixtures and pure He was performed with the optical setup shown in Figure 12. Radiation emerging from the test section through the unsupported area of the fused quartz window was focused by quartz lenses 1 and 2 at the slit of the stigmatic Bausch and Lomb medium quartz prism spectrograph in such a way that the spectrograph collimator lens was filled. The front surface mirror was mounted on a rotary table so that it could be turned 90° to direct the radiation toward a monochromator for another type of experiment described below.

Immediately in front of the spectrograph slit a high speed shutter (Reference 6) was mounted for time-resolved spectroscopy. This shutter consists of a slotted plate driven quickly past the spectrograph slit in such a way that light can enter the slit only during the short interval when the slot is aligned with the slit. Shutter open times are controlled by varying the energy stored in

the capacitor discharge unit which activates the driving mechanism. The shutter open time is synchronized with the time of maximum pressure and temperature in the test section by triggering the capacitor discharge at a predetermined value of the voltage analog of the pressure generated by the quartz crystal pressure transducer located in the end-plug of the test section. A pulse from the trigger unit is superimposed on the pressure signal to indicate the initiation of shutter action. Further details of shutter action, calibration, and associated electronics can be found in Reference 6, and details of the pressure recording instrumentation can be found in Reference 7.

Because the compressor is free to move rearward as the piston travels forward, there is only a short period of time during which the quartz window is in alignment with the optical axis of the spectrograph. The compressor motion is monitored by a precision linear motion potentiometer whose output as a function of time is displayed on the oscilloscope along with the pressure signal. It was found that by properly prepositioning the compressor, the window will come into alignment and be relatively stationary during nearly the entire first compression cycle. A typical motion and pressure record is shown in Figure 18(a).

Spectra were recorded on Kodak 103-F emulsions which are sensitive from 2000 Å to 7000 Å and on Kodak I-N emulsions which extend the detection range to 9000 Å. Typical exposure times were of the order of 300 microseconds and slit widths varied from 100 to 25 microns. Films were developed in Kodak D-19 for 4 minutes at 20°C in a temperature regulated processor. Emulsion calibrations were performed using a step slit uniformly illuminated by carbon arc radiation for submillisecond exposure times to minimize reciprocity failure. Heterochromatic photometry was accomplished using the carbon arc as a standard light source and assuming that the anode crater of the arc radiated as a 3800°K blackbody. The arc used is

identical to the arc described in Reference 8, and National Carbon Co. $\frac{1}{4}$ inch type SPK anodes were used. The arc radiation was passed through the same optical paths as that followed by the compressed gas radiation.

2.3.3 Absorption Experiments

Measurements of absorption coefficients can be made in a relatively straightforward manner by passing a beam of light through the gas sample under study. The relevant physical theory is briefly reviewed below.

If the gas sample can be assumed to be uniform in temperature, density, and chemical composition, we can use Beer's Law:

$$I = I_o e^{-\tau}, \tag{1}$$

where τ is the dimensionless quantity called optical depth or optical thickness; I_o is the intensity of the test beam as it enters the gas sample, and I is the emerging, attenuated intensity of the beam after it has traversed the sample. The optical depth is often expressed as:

$$\tau = k\ell, \tag{2}$$

where k is the absorption coefficient (and includes the effect of induced emission), and ℓ is the path length or thickness of the sample. The microscopic properties of the absorbing gas render τ wavelength dependent, and, therefore, the experiment must be done monochromatically.

Figure 13 illustrates the optical scheme designed and constructed for absorption experiments. Light from the carbon arc anode crater mentioned above is focused at the plane of the chopper by quartz lens L_4, and is then refocused by quartz lens L_3 at the center of the test section. The beam traversing the test section is narrow, having a maximum diameter of 5 millimeters. Quartz lens

L_1 forms a magnified image of the anode crater at the mask which has a circular aperture small enough to pass only the rays originating from the central, uniformly luminous portion of the anode crater. Quartz lens L_5 images the mask aperture at the slit of the Littrow mounted plane grating monochromator (Reference 9) in such a way that the collimating mirror of the monochromator is filled with light. The photomultiplier tube housing was modified to accept an RCA 7200 photomultiplier tube which is sensitive from 1800 Å to 6000 Å with peak sensitivity in the 3000 Å - 4000 Å region. This tube was operated at somewhat less than maximum photocathode potential to reduce the noise level, and its output was amplified by an emitter follower, impedence matching circuit before being displayed on an oscilloscope. Linearity of photomultiplier response was checked by a method similar to that described in Reference 10. The half-width of the slit function of the monochromator was 3 Å for all the experiments discussed here.

Because the compressed gas itself often radiates, precautions must be taken in order to separate the signal due to the attenuated test beam from that due to the self-luminosity of the gas sample. This function is performed by the slotted drum chopper which interrupts the test beam before it enters the test section. The chopper is driven by a high-speed grinder motor and spindle at rates up to 3500 rpm, and typically produces a series of "square" light pulses of 100 microseconds duration with intervals of 150 microseconds between pulses. At the instant when the chopper is going from its closed to open position, the detector signal goes from that due to the compressed gas alone to that due to the sum of compressed gas radiation and attenuated test beam radiation, so subtraction yields the test beam signal at that instant, and a corresponding datum can be obtained at the instant the chopper closes. The duration of each chopper "pulse" is short compared to the duration of the gas compression cycle, and, therefore, the opacity of the gas sample can be followed during most of the compression cycle, and, consequently, over a wide range of pressures and temperatures

during a single compressor run. However, the present spectroscopic instrumentation allows opacity measurements at only one wavelength per run.

A further refinement of the optical scheme shown in Figure 13 involves the use of the diaphragm at lens L_1. The gas radiation beam subtends at lens L_1 a larger solid angle than does the carbon arc beam. Therefore, by stopping down this lens to the point where the extreme rays of the carbon arc beam just begin to be intercepted we are assured that the aperture in the mask subtends equal solid angles of both carbon arc radiation and compressed gas radiation. The signals due to carbon arc radiation and to gas radiation can then be directly compared. Furthermore, if the radiation from a standard light source, such as a blackbody or a calibrated tungsten lamp, can be passed through the same optical train as does the gas radiation, then such a calibration will permit intensities to be measured in absolute units.

3.0 EXPERIMENTAL RESULTS

3.1 Pure Hydrogen Experiments

Survey spectra were made by compressing pure H_2 from an initial pressure of one atmosphere up to maximum pressures of 2315 atmospheres. The intent was to search for emission spectral features for which opacity measurements could then be made.

A single Teflon cup seal was used on the piston to prevent forward leakage of the helium driver gas, and the molybdenum piston head was used. Wide slit widths of 100 microns were used, and the high-speed shutter was not employed in these experiments, thereby enhancing the probability of detection.

No spectra could be detected in these pure H_2 experiments. At the maximum pressure attained, the calculated gas temperature was approximately 2700°K and the degree of dissociation was approximately 0.1%. It was found that the piston face came to within 3 millimeters of the end-plug at these pressures. Such a small separation made attempts to attain higher pressures and temperatures with pure H_2 risky, and precluded the possibility of absorption measurements using the test beam of 5 millimeter diameter cross-section. Additional experiments with pure H_2 test gas have been postponed until means are found to increase the volume of the compressed gas sample.

3.2 Hydrogen/Helium Mixture Experiments

As indicated above in section 2.2, appreciable concentrations of both H_2 and H can be produced at high pressures and temperatures by compressing a mixture of hydrogen and a monatomic gas such as argon or helium. If the monatomic gas concentration is high, the thermodynamics of the compression process is largely controlled by the adiabatic exponent of the monatomic gas, and, consequently, for a given pressure, the gas temperature will be higher than for compression of a pure diatomic gas. The principal result of such a mixture experiment is a quantity of partially dissociated diatomic gas immersed in a monatomic gas heat bath.

Helium was chosen for the monatomic gas for several reasons. At a given temperature and pressure, it supplies fewer electrons to the mixture than any other gas. It will not contribute any important sources of opacity except for its role in broadening spectral lines, and even in this role it is the least effective of all foreign gases because of its extremely small polarizability. It produces small and often negligible wavelength shifts in collisional line broadening processes, and thus the peak of a spectral feature can be expected to remain within the frequency passband of the monochromator during the entire compression cycle. The compression

process using helium is free from the affects of shock waves which are often found in the compression of other gases which have slower sound velocities.

3.2.1 Emission Experiments with Mixtures

Preliminary mixture experiments with 20/80 and 10/90 hydrogen/helium mixture ratios were performed using time-integrated spectroscopy and wide slit widths for survey purposes. These spectra revealed metal impurity lines, some OH bands, and background continua extending from the red limit of 103-F emulsion sensitivity (7000 Å) to approximately 2200 Å in the ultraviolet. These spectra were not greatly different from earlier spectra recorded with this and an earlier compressor at lower pressures using pure helium as the test gas except that on a shot which attained 3170 atmospheres and a calculated temperature of 6500°K, using a 10/90 mixture ratio, the metal lines appeared quite weak superimposed on a very strong continuum.

Subsequent emission experiments consisted of a careful attempt to produce two spectrograms on the same emulsion, at the same exposure time and slit width, and at the same values of calculated temperatures, with one spectrogram displaying the spectra from a pure helium compression, the other showing the results of a 10/90 mixture ratio. The resulting spectrograms are shown in Figure 14. The experimental conditions for these two spectra are as follows: 103-F emulsion, high speed shutter exposure times = 300 microseconds, slit widths = 25 microns. The measured pressures, calculated temperatures and compositions are, for the pure He spectra: average pressure during the shutter open time, P_{ave} = 1830 atmospheres, average temperature, T_{ave} = 6040°K, average helium density, $N_{He} = 2.2 \times 10^{21} cm^{-3}$. For the 10/90 mixture ratio spectra: P_{ave} = 2630 atmospheres, T_{ave} = 6160°K, and $N_{He} = 2.6 \times 10^{21} cm^{-3}$, $N_{H_2} = 1.6 \times 10^{20} cm^{-3}$, and $N_H = 2.5 \times 10^{20} cm^{-3}$. Electron

concentrations are, for the pure helium experiment, $N_e = 2 \times 10^{11} cm^{-3}$ from the ionization of helium, and, for the 10/90 mixture ratio experiment, $N_e = 1.2 \times 10^{15} cm^{-3}$; in both cases, ionization of metal vapors may make significant contributions to N_e.

Each of the compressor spectra in Figure 14 has narrow mercury lines superimposed for wavelength calibration, a rough wavelength scale is shown in the lower strip, and the upper three narrow spectra are the carbon arc exposures used for standardization in the heterochromatic photometry procedure mentioned earlier. Figure 15(a), (b), (c), (d), and (e) show densitometer tracings of the 10/90 mixture ratio spectra shown in Figure 14. These traces show photographic density versus wavelength on non-linear scales and line identifications for both the narrow mercury lines and the most prominent metal impurity lines. Most of the lines not identified on these charts are lines of Fe I. The metal vapors producing these lines come from various compressor parts exposed to hot gas during the compression cycle. The large arrows on these charts indicate regions where background continuum intensity measurements have been made on both spectra displayed in Figure 14.

The results of the intensity measurements are displayed in Figure 16. The measurements are obtained by means of conventional emulsion calibration and standardization procedures, and the intensities obtained from each spectrogram can be compared directly because of identical optics, exposure times, and slit widths. It is difficult to determine accurately the errors present in photographic photometry because of the numerous steps in the data reduction process. The most accurate and painstaking photographic intensity measurements yield errors of the order of ±2% (see Reference 11). Because of the possible presence of such effects as reciprocity failure and the Eberhard effect, weak molecular bands in the carbon arc standardization spectra, and uncertainty in the carbon arc temperature, it is felt that the data in Figure 16 are accurate to within ±15%, except the points at 3330 Å for which the

errors are larger because of an additional uncertainty in the placement of the 3330 Å emulsion calibration curve relative to the curves for the other wavelengths due to the almost undetectable intensity of the carbon arc at that wavelength. The fundamental problem of locating the true continuum level in the presence of many broadened spectral lines will be treated in a later section.

The final emission experiment performed was a survey spectrogram made from a 10/90 mixture ratio at nearly the same pressure and temperature as that for the 10/90 mixture ratio spectra displayed in Figure 14, except it was made on a Kodak I-N emulsion sensitive to near-infrared wavelengths as well as to visible and ultraviolet radiation. The resonance "D" lines of potassium (an everpresent impurity) at 7665 and 7699 Å appeared blended and one of the resonance "D" lines of cesium at 8521 Å was identified near the long wavelength cutoff for this emulsion. These lines were superimposed on a weak continuum, but the wavelength resolution of the prism spectrograph is so poor in this spectral region that intensity measurements were deemed impractical.

3.2.2 Absorption Experiments with Mixtures

The opacity measuring technique described above was first tested at moderate pressures with pure helium test gas, and with the monochromator set at the peaks of several prominent metal impurity lines. These experiments not only enabled operational checks of the scheme to be made, but also allowed estimates of the abundance of impurity metal vapors to be made.

One operational difficulty was apparent upon inspection of the first few records of the chopped photomultiplier signal, namely, an apparent source of opacity made an appearance several milliseconds after the first compression and expansion of the test gas, but, nevertheless, before the optical alignment was destroyed by compressor motion. This apparent opacity was found to have no

wavelength dependence, nor was it found to be fully reproducible, and its cause was finally found to be a small jet of gas and dust near the unsupported area of the window. This small dust cloud obstructed the carbon arc beam causing attenuation of its intensity. Although this delayed attenuation did not interfere with opacity measurements during the times of maximum test gas pressure and temperature, it was effectively removed at moderate peak pressures by cementing the windows to their supports with a rubber base adhesive which also served to cushion the window and inhibit window breakage. The present cementing procedure does not fully eliminate the delayed attenuation at high pressures, however.

After adopting the cementing procedure, absorption experiments were performed with the monochromator set at the peaks of the sodium and calcium resonance lines. The records for these lines are shown in Figures 17 (a) and (b). These figures show pressure as a function of time on the upper halves of the photographs and the chopped photomultiplier output on the lower halves. For both these records, two major vertical divisions of deflection corresponds to I_o in Equation (1). The envelope of the tops of the pulses corresponds to the sum of attenuated test beam intensity and the intensity of the gas radiation; the envelope of the bottoms of the pulses is the gas radiation intensity alone as a function of time. The fluctuations occurring well after the pressure pulses are due to the onset of destruction of optical alignment.

From measurements of Figure 17 (a), and after correcting for the opacity in the continuum under the line in a separate experiment, the opacity at the peak of 4226.7 Å resonance line of neutral calcium was found to be: $\tau = 0.34$. The measured maximum pressure for that shot was 750 atmospheres with a calculated temperature of 4220°K, and calculated helium density of $N_{He} = 1.3 \times 10^{20} cm^{-3}$. The relation between opacity and the density of absorbing atoms is (Reference 12):

$$\tau = \pi r_o f N_n \ell \left(1 - e^{-h\nu/kT}\right)\left[\frac{W}{(\Delta w)^2+W^2}\right], \qquad (3)$$

where r_o is the classical electron radius and is 2.82×10^{-13}cm., f is the oscillator strength, N_n is the number of atoms in the lower state of the line, ℓ is the path length, $(1 \quad e^{h\nu/kT})$ is the induced emission term and where $h\nu$ is the absorbed photon energy, Δw is the distance from the line center in units of cm^{-1}, and W is the half half width of the assumed Lorentzian broadened line in units of cm^{-1}. The value of W is taken from the line broadening data of Hindmarsh (Reference 13). Substitution of the experimental data for this shot yields a calcium abundance of $N_{CaI} = 8.5 \times 10^{11} cm^{-3}$. A similar calculation for the blended sodium "D" lines from the data of Figure 17 (b) yields a sodium abundance of $N_{Na} = 1.0 \times 10^{12} cm^{-3}$.

Figure 18 (a) illustrates a pressure-time record for a pure helium shot for which the initial conditions and maximum pressure are identical to the shot that produced the pure helium spectrogram in Figure 14, and the pure helium intensity data in Figure 16. Also shown on this record is the output of the motion transducer, the slightly curving line just below the central gradicle line which serves to indicate the exact alignment position of the center of the side window with the axis of the external optics. Exact alignment during the entire pressure pulse was achieved to within 0.050 inch, a negligible error.

Figure 18 (b) displays the chopped output of the monochromator-photomultiplier at a wavelength of 5000 Å for this pure helium shot at a maximum pressure of 1890 atmospheres and calculated temperature of 6080°K. At this wavelength, the spectra of Figure 14 shows only continuum radiation. Using equation (1) for Figure 18 (b) at maximum conditions, the opacity was found to be $\tau_{5000\ \text{Å}} = 0.39$.

4.0 DISCUSSION AND CONCLUSIONS

The principal findings of this investigation are the continua intensities shown in Figure 16, the opacity measurement at 5000 Å in the pure helium experiment, and the absence of any bound-bound Balmer line opacity. The failure to detect emission features in pure hydrogen is undoubtedly due to the low gas temperatures and short observation times. Although the red wing of the Lyman alpha (L_α) transition and the effects of such mechanisms as pressure-induced transitions in molecular hydrogen might have been observable in absorption, such experiments must await compressor modifications which will result in larger compressed test gas volumes.

This section of the report suggests possible mechanisms which may explain the observed wavelength dependence of the continua. It is felt that, due to the presence of the impurity lines, the precision of the measurements is not high enough to permit resolution of small scale fluctuations in the continua curves. However, the measurements are reliable enough to permit the following observations.

The intensity of the pure helium continua is greater than that for the 10% hydrogen mixture over the wavelength range of 3300 Å to 6300 Å by a factor ranging from 2 to 3. If both continua arise from the same mechanism, this fact may be explainable by a temperature difference between the two experiments and a resulting difference in the abundance of the continuum producers.

The intensity of both continua increases with decreasing wavelength. In view of the fact that both continua exhibit the same general properties, it is possible they both arise from the same mechanism. Since helium is the major constituent of both gas mixtures several helium related mechanisms should be considered.

Molecular radiation from He_2. Although this molecule shows several bands in the visible and ultraviolet parts of the spectrum, their position does not correspond with that of any features in the compressor spectra. Furthermore, since the ground state of He_2 is unstable, a very high gas temperature is required to produce the excited He atoms which form He_2.

Negative He ion, He^-. This ion exists and has an electron binding energy of 0.075 eV (Reference 14). Its only bound state is metastable and is 19 eV above the He ground state, so that only free-free transitions are of interest here. However, the free-free absorption coefficient for He^- increases toward longer wavelengths (Reference 15) and cannot be a suitable candidate here.

Two other possible continuum mechanisms are associated with the impurities present in both mixtures.

Metallic negative ions. In addition to He^- (and the well known H^-) many metals form negative ions whose binding energies and continuum absorption cross-sections are of the same order of magnitude as those for H^- (Reference 16). The most likely candidate among the metallic negative ions as a possible source of the observed continua is Cu^-. Its binding energy of 1.80 eV (Reference 17) results in a threshold wavelength of approximately 6880 Å with intensity increasing toward the UV, and is possibly high enough to shift the peak of its bound-free absorption coefficient to wavelengths shorter than 4000 Å. A small amount of copper vapor is produced in the compressor by the heating of the phosphor-bronze piston body and window jackets by the hot test gas.

Many broad, weak, impurity lines. Systematic errors in measurements of continuous background intensities are often caused by the presence of many broad, weak, impurity lines with overlapping wings. In the compressor spectra presented here, several Fe I multiplets

have been identified, and in view of the fact that the Fe I spectrum has many closely spaced lines in the blue and near ultraviolet parts of the spectrum, these relatively weak, broadened lines may constitute a pseudo-continuum which may partially account for the intensity increase with decreasing wavelength.

The experiments performed to date do not reveal whether the continua of Figure 16 originate from the same or from quite different mechanisms. Although helium is the major constituent of both gas mixtures, the compositions of the two mixtures are quite different. There are 10^{20} hydrogen molecules and atoms per cubic centimeter, as well as 4 orders of magnitude greater electron density in the 10/90 H_2/He mixture. Therefore, in addition to the above mechanisms which may explain the pure helium continuum, the following mechanisms must be included in a discussion of the hydrogen mixture continuum.

Negative hydrogen ion, H^-. This well-known source of opacity at moderate gas temperatures has a bound-free absorption coefficient which peaks in the near infrared and a free-free absorption coefficient which is too small to be of interest in the wavelength range of this study. Consequently, it alone cannot account for the properties of the observed hydrogen mixture continuum.

Red wing of the Lyman alpha (L_α) line. Pressure broadening of the spectral lines of atomic hydrogen can be employed to increase the opacity of the gas. The best "foreign gas" additive (i.e., perturber) for broadening the L_α line is atomic hydrogen. This type of broadening, commonly called resonance or self-broadening, occurs when the upper or lower level of a spectral line has an allowed dipole transition to the ground state, and when the absorbing atom is surrounded by like atoms in the ground state. In the range of pressure and temperature where the impact theory of spectral line broadening is valid, this broadening mechanism produces an unshifted, temperature insensitive, Lorentzian line whose half-width is

proportional to the atomic hydrogen density. Van der Waals broadening, on the other hand, occurs when the absorbing atom is surrounded by unlike atoms, i.e. with H_2 or He. This broadening mechanism is much less important than resonance broadening, and can be neglected.

Although the peak of L_α occurs at 1216 Å, the high density of hydrogen atoms used in these experiments may result in an intense, long wavelength wing with detectable opacity in the near ultraviolet and visible spectrum. Unfortunately, uncertainties in the line broadening theory at such large distances from the line center and at such high densities, coupled with uncertainties in the atomic hydrogen abundance in the compressor experiments, do not permit this possible opacity source to be either disregarded or treated in fuller detail at this time.

To summarize then, the findings of this investigation, hydrogen/helium mixtures were compressed to pressures and temperatures exceeding 2500 atmospheres and 5000°K, and the resulting emission was recorded in the wavelength range of 2000 - 9000 Å and analyzed. Although the discrete spectra that were observed could not be ascribed to hydrogen, the continuum may have contributions attributable to hydrogen. The strong continuum that was observed in the pure helium experiments, continuum due to helium and metal impurities, and present in the mixtures experiments in an unknown amount, precludes a determination at this time of the role that hydrogen plays in the formation of the continuum observed in the mixtures experiments.

REFERENCES

1. Lalos, G. T., "Laboratory Production of Hot, Dense Gases," Rev. Sci. Instr. 33,214, 1962.
2. Lalos, G. T. and Hammond, G. L., "Emission Spectra of Hot, Dense Gases," Astroph. J. 135,616, 1962.
3. Hammond, G. L., "The Shift and Broadening of the Resonance Doublet of Ba II Caused by He and Ar Collisions," Astroph. J. 136,431, 1962.
4. White, W. B., Johnson, S. M., and Dantzig, G. B., "Chemical Equilibrium in Complex Mixtures," J. Chem. Phys. 28,751, 1958.
5. Burke, B. A., and Lalos, G. T., "Ionic Equilibria in Hot, Highly Compressed Gases," NOLTR 65-64 (in preparation).
6. Kendall, P. A., "High Speed Electromechanical Shutter for Time Resolved Spectroscopy," Applied Spectroscopy 18,33, 1964.
7. Kendall, P. A., "NOL 100,000 psi Adiabatic Compressor, Electronic Instrumentation," NOLTN-4541, 1958.
8. Null, M. R. and Lozier, W. W., "Carbon Arc as a Radiation Standard," JOSA 52,1156, 1962.
9. Diffraction Products, Inc., Model S-05-02, distributed by Engis Equipment Co., Chicago, Ill.
10. McLean, E., et al, "Spectroscopic Study of Helium Plasmas Produced by Magnetically Driven Shock Waves," Phys. Fluids 3,843, 1960
11. Wright, K. O., "Spectrophotometry," in Astronomical Techniques, W. A. Hiltner, ed., Chicago Univ. Press 1962, Chapt. 4.
12. Griem, H. R., Plasma Spectroscopy, McGraw-Hill Book Co., New York 1964, Chapt. 7.
13. Hindmarsh, W. R., "Collision Broadening and Shift in the Resonance Line of Calcium," Monthly Notices Roy. Astron. Soc. 119,11, 1959.
14. Smirnov, B. M., "Atomic Negative Ions," High Temperature 3,716, 1965; English translation by Consultants Bureau/ Plenum Press, New York, of Teplofizika Vysokikh Temperatur 3,775, 1965.

REFERENCES (Cont'd)

15. Somerville, W. B., "The Continuous Absorption Coefficient of He^-," Astroph. J. 141, 811, 1965.

16. Branscomb, L. M., in D. R. Bates (ed.), Atomic and Molecular Processes, Academic Press, Inc., New York 1962, Chapt. 4.

17. Clementi, E., "Atomic Negative Ions: The Iron Series," Phys. Rev. 135, A 980, 1964.

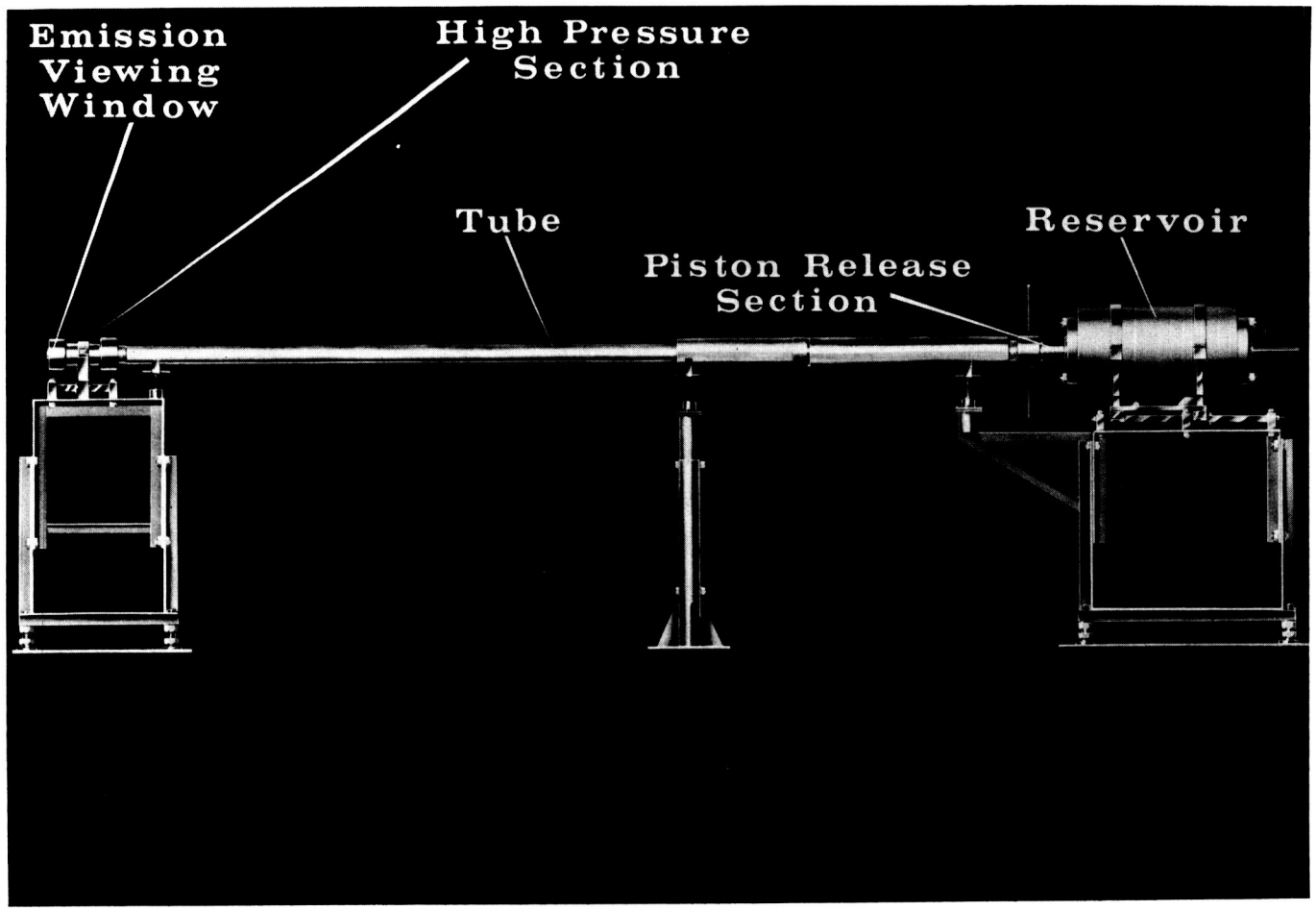

FIG. 1 BALLISTIC PISTON COMPRESSOR

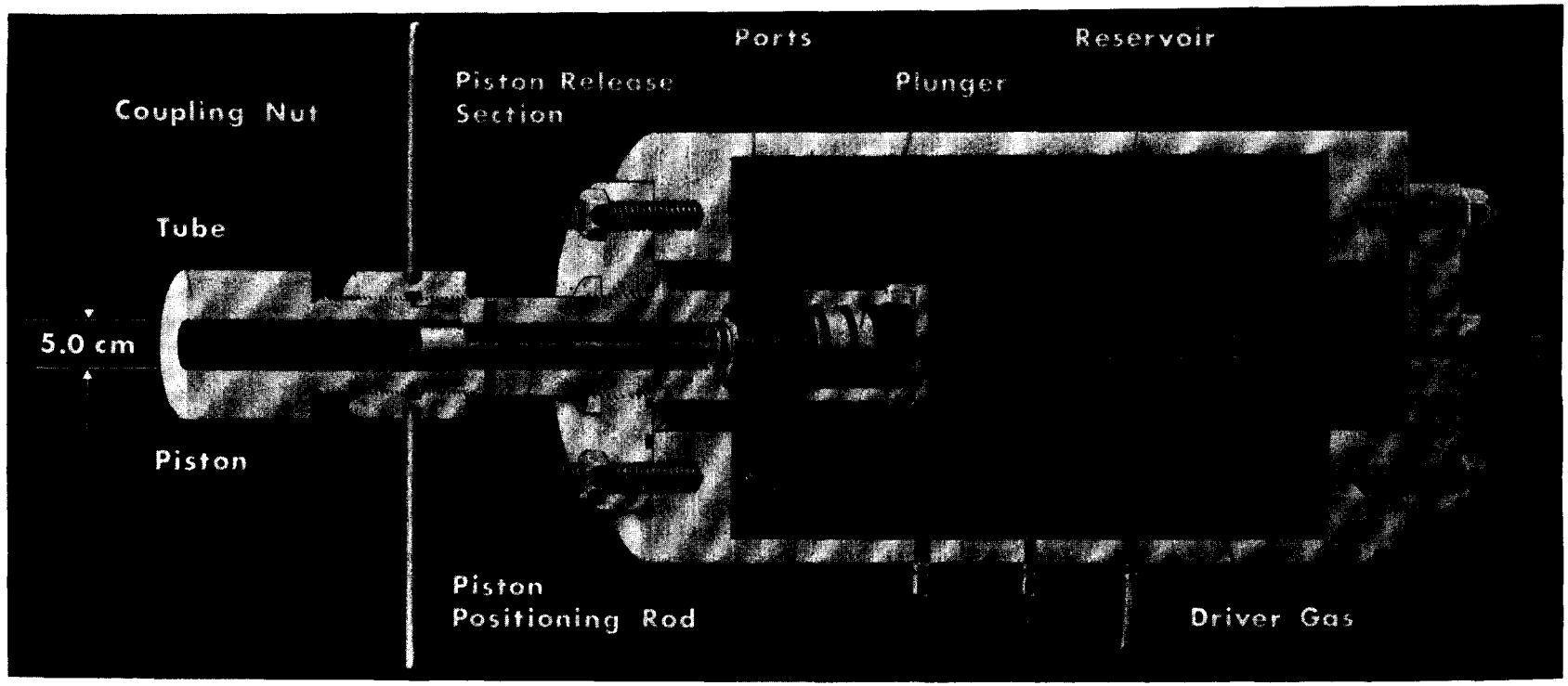

FIG. 2 BALLISTIC PISTON COMPRESSOR (RESERVOIR END)

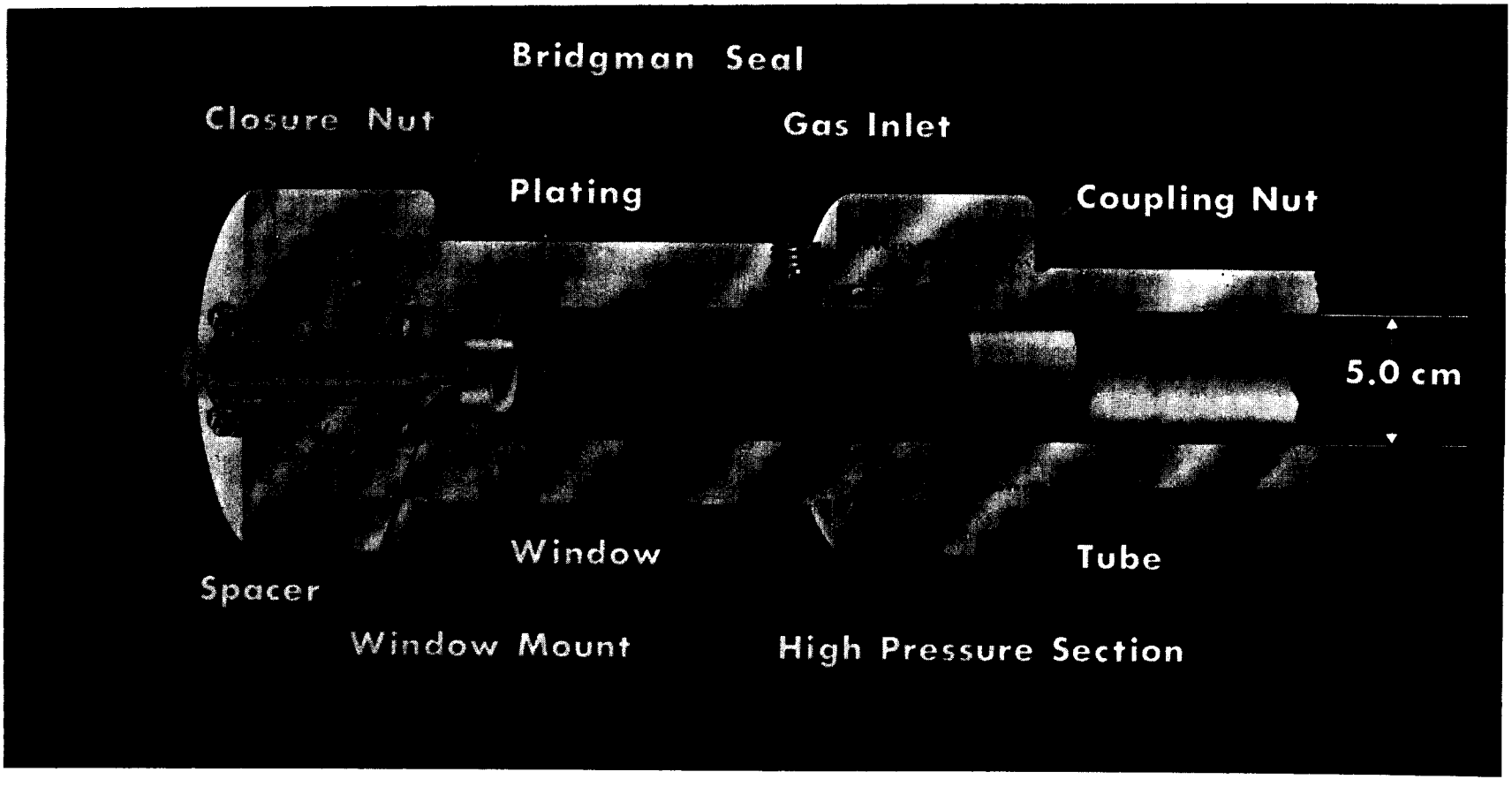

FIG. 3 BALLISTIC PISTON COMPRESSOR (HIGH PRESSURE END)

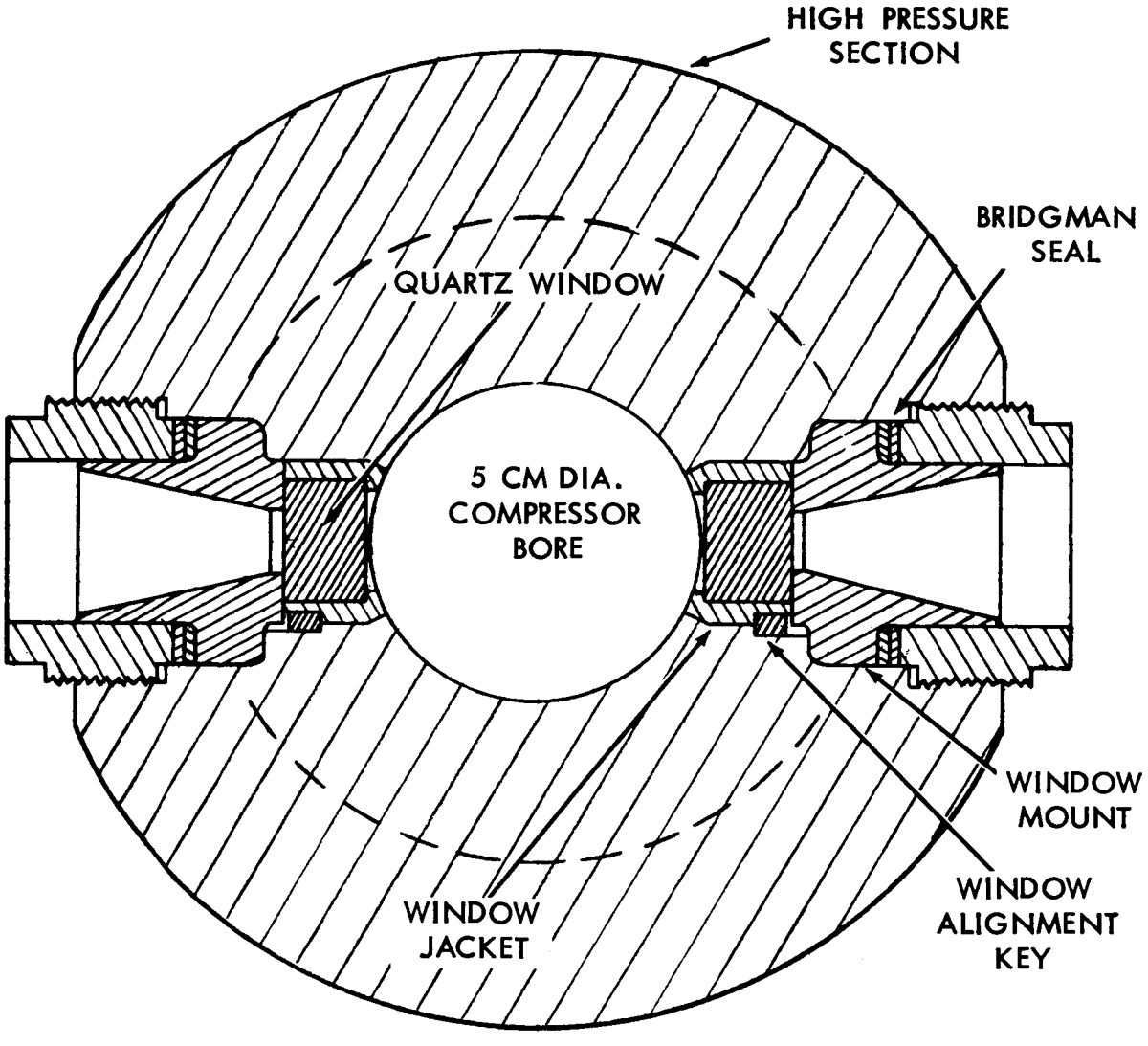

FIG. 4 DETAILS OF SIDE WINDOW TEST SECTION

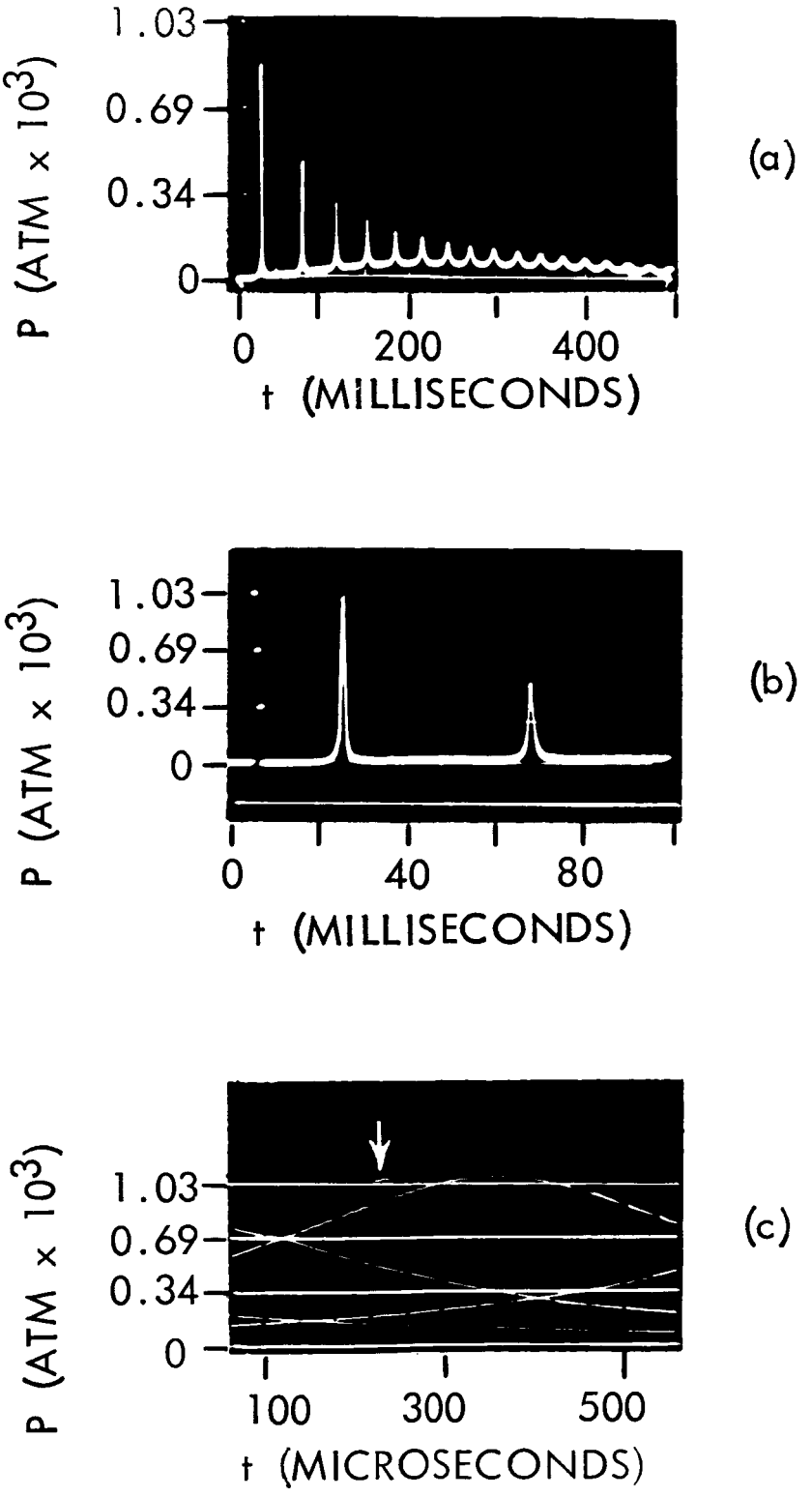

FIG. 5 OSCILLOSCOPE RECORD OF TEST GAS PRESSURE VERSUS TIME

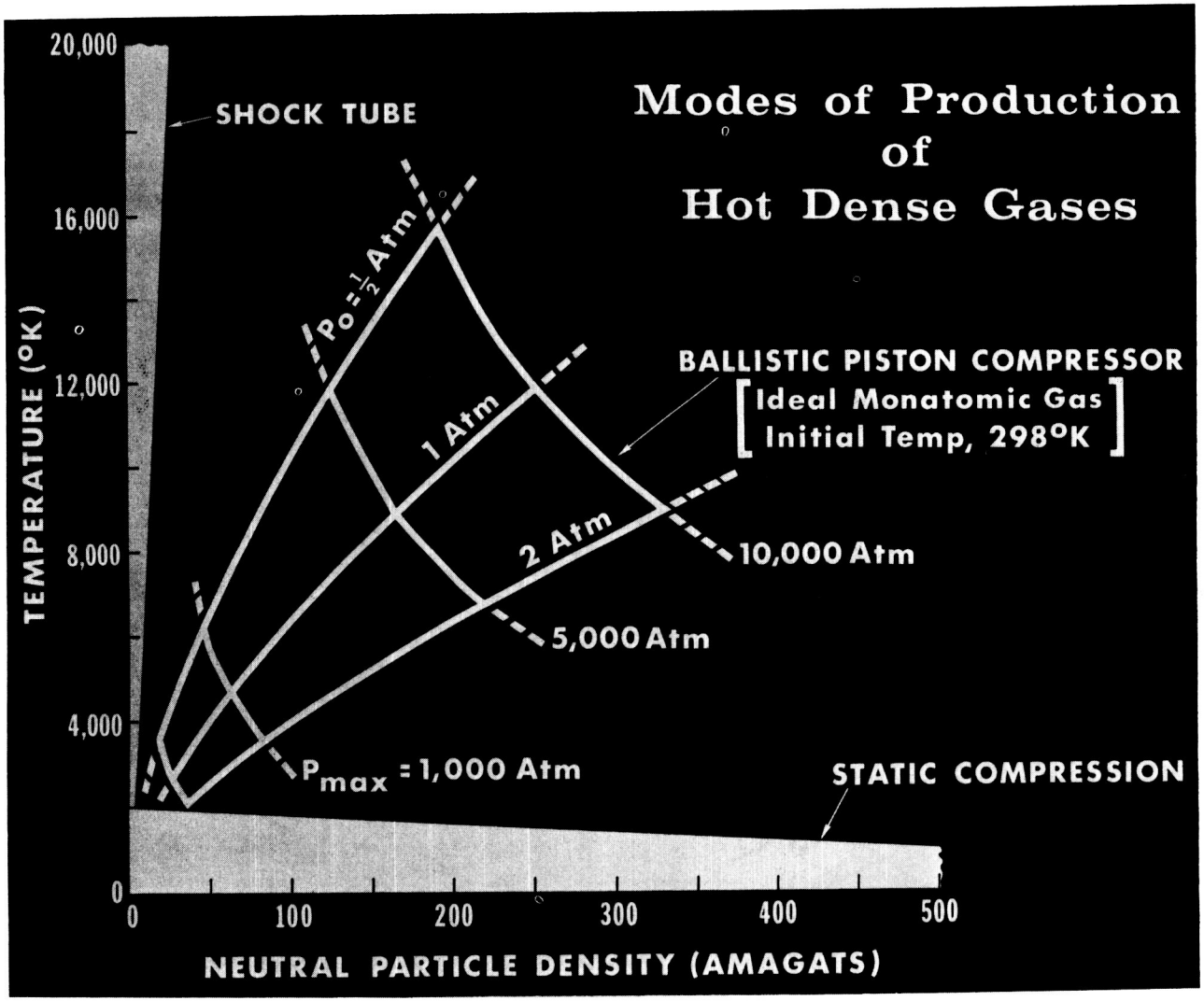

FIG. 6 TEMPERATURE VERSUS NEUTRAL PARTICLE DENSITY

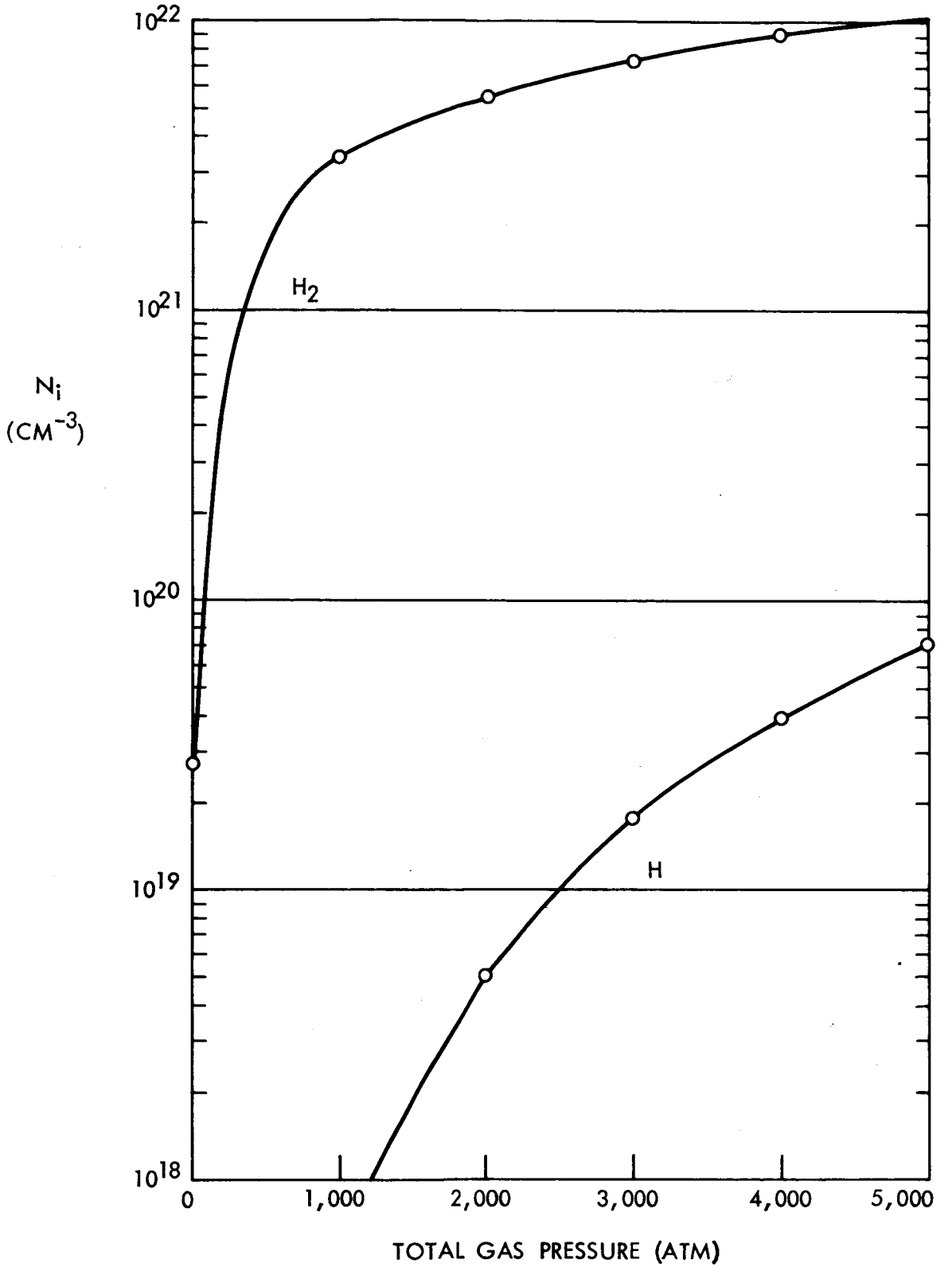

FIG. 7 PARTICLE DENSITY VERSUS PRESSURE FOR PURE H_2. INITIAL CONDITIONS: $P_o = 1$ ATM, $T_o = 298°K$

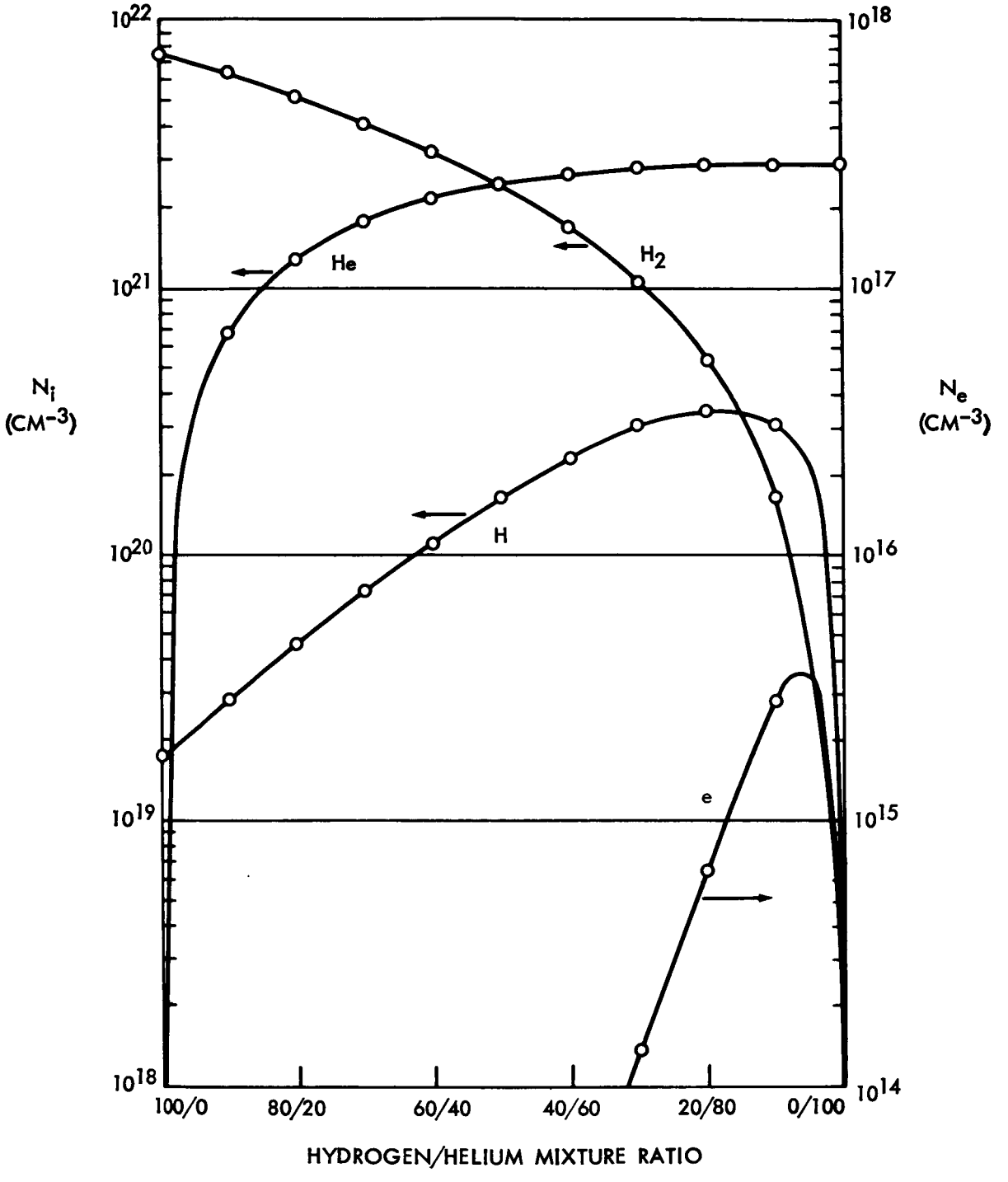

FIG. 8 PARTICLE DENSITY VERSUS MIXTURE RATIO FOR P = 3000 ATM. INITIAL CONDITIONS: P_o = 1 ATM, T_o = 298 °K

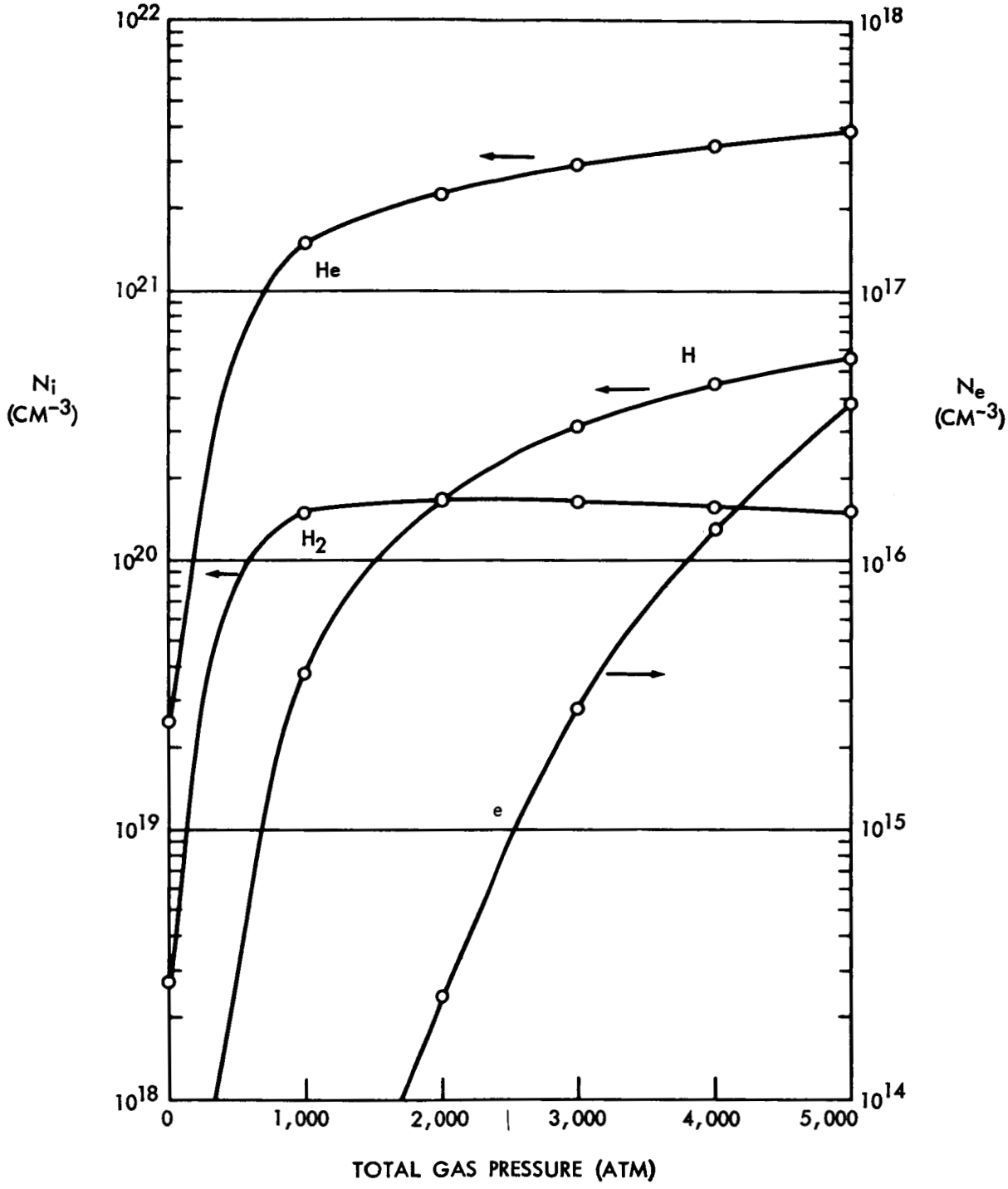

FIG. 9 PARTICLE DENSITY VERSUS PRESSURE FOR 10/90 H_2/He MIXTURE RATIO. INITIAL CONDITIONS: P_o = 1 ATM, T_o = 298 °K

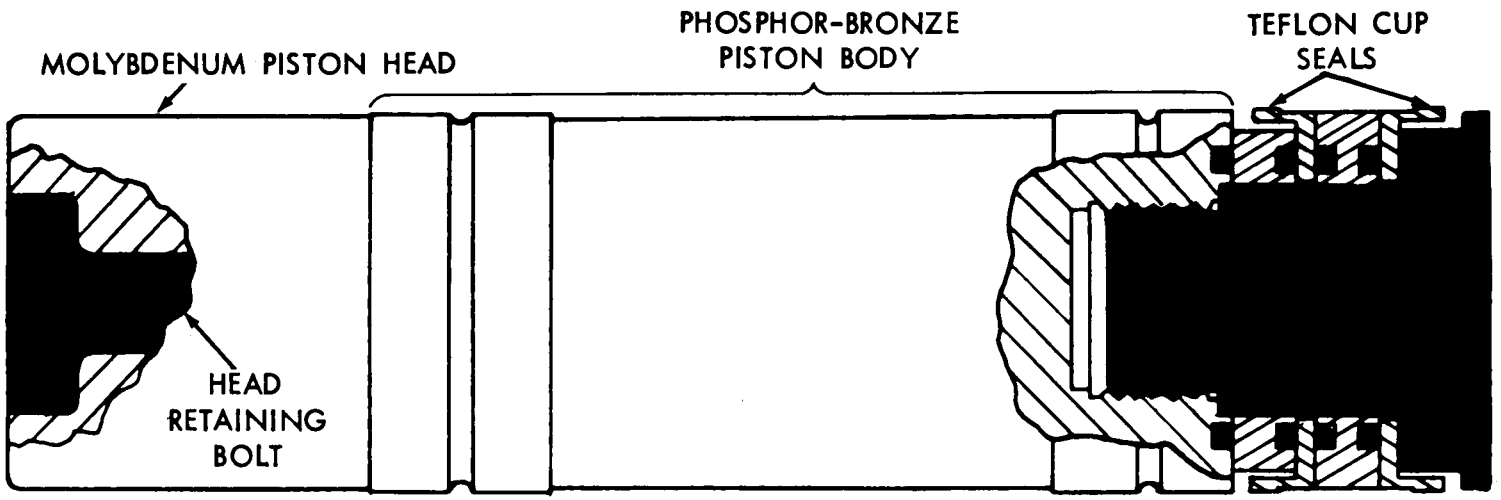

FIG. 10 PISTON WITH SEALS AND HIGH TEMPERATURE RESISTANT HEAD

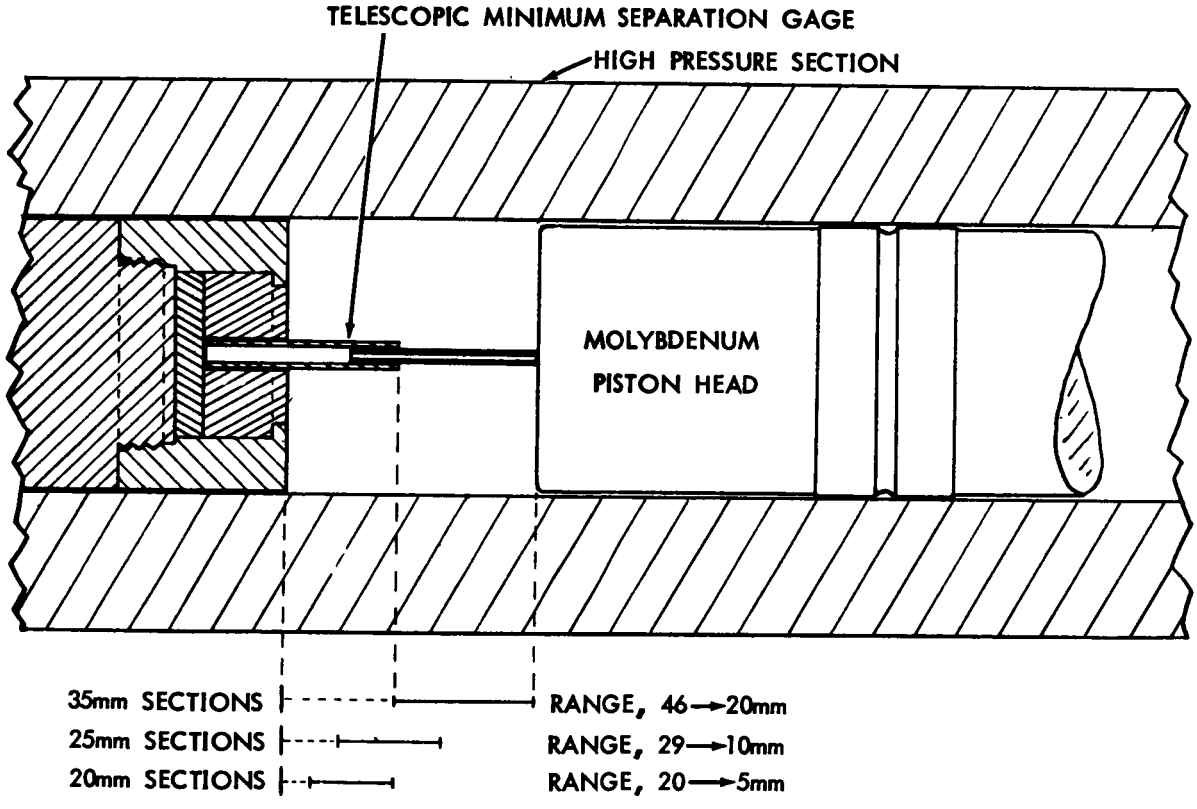

FIG. 11 TELESCOPIC MINIMUM SEPARATION GAGE

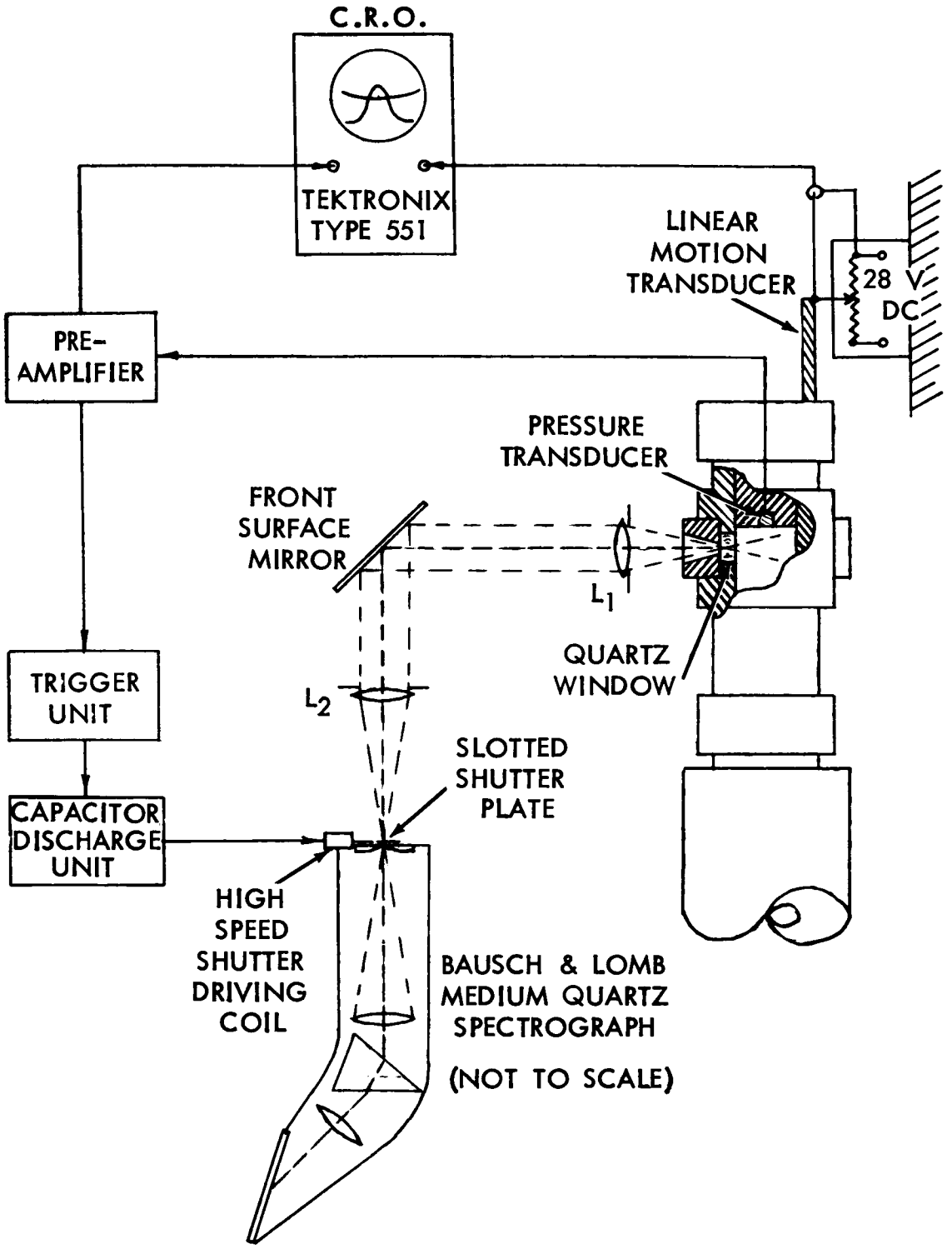

FIG. 12 OPTICS FOR EMISSION EXPERIMENTS

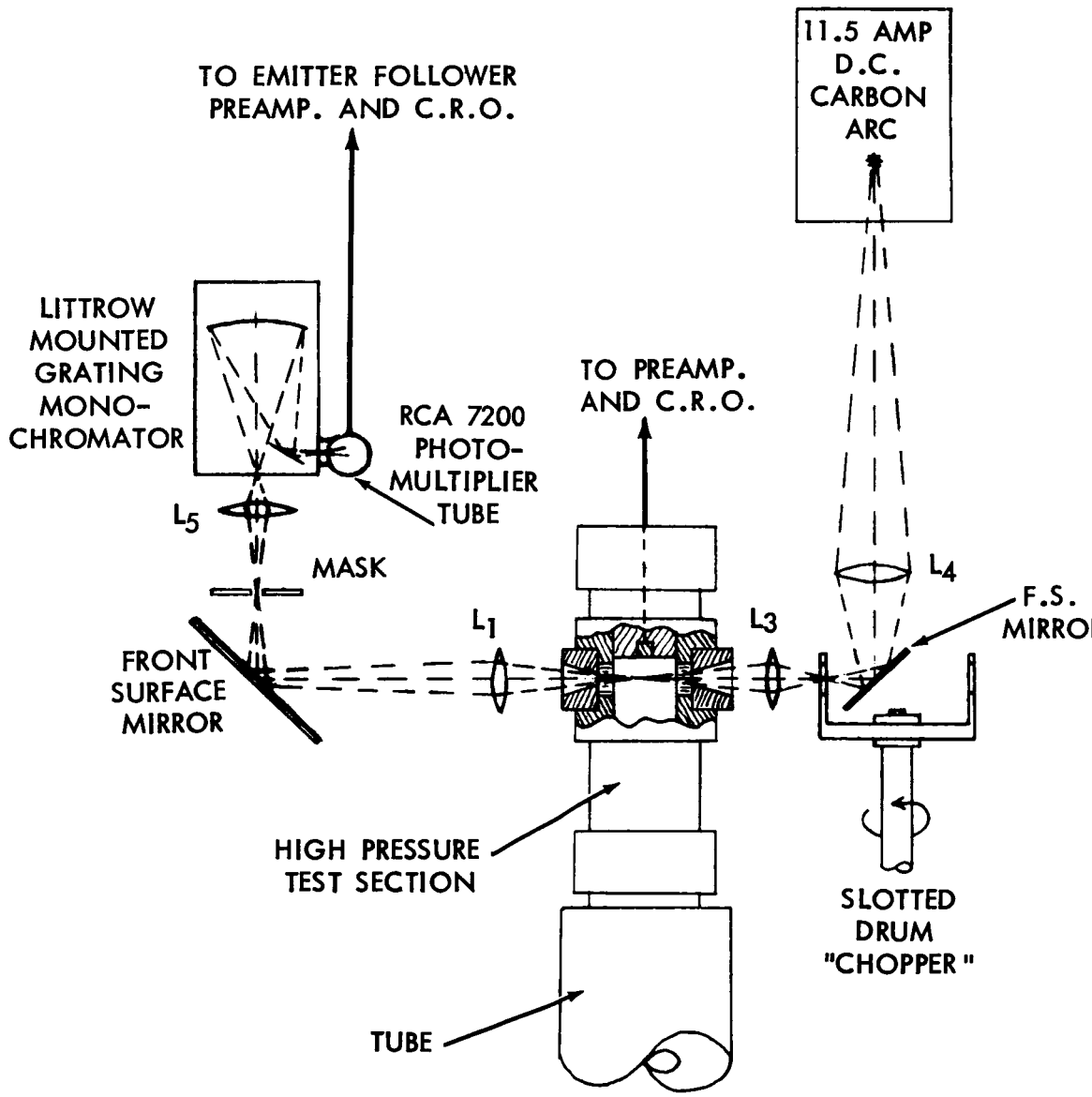

FIG. 13 OPTICS FOR ABSORPTION EXPERIMENTS

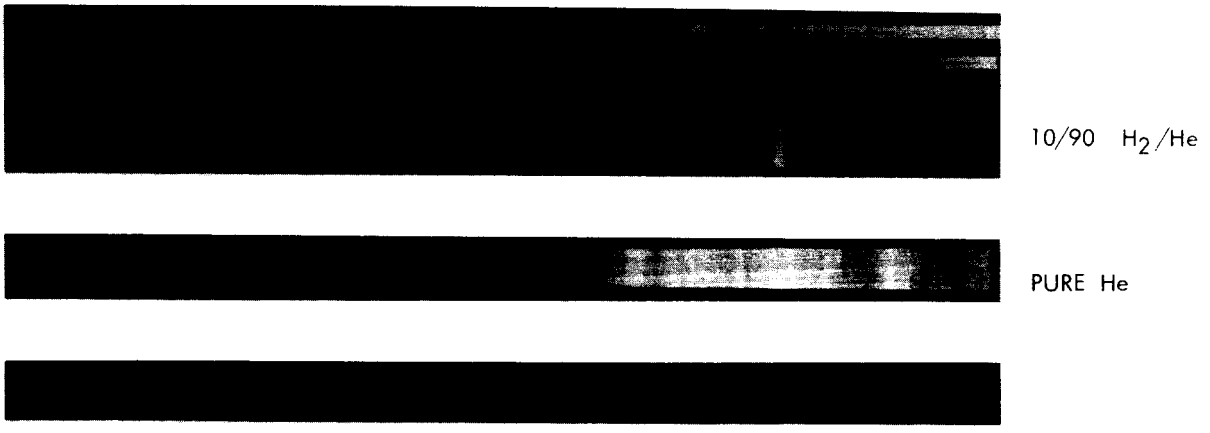

FIG. 14 TIME RESOLVED SPECTRA FOR PURE HELIUM AND 10% HYDROGEN MIXTURE AT 6000 °K 103-F PLATE, 25 μSLIT, 300 μSEC EXPOSURE

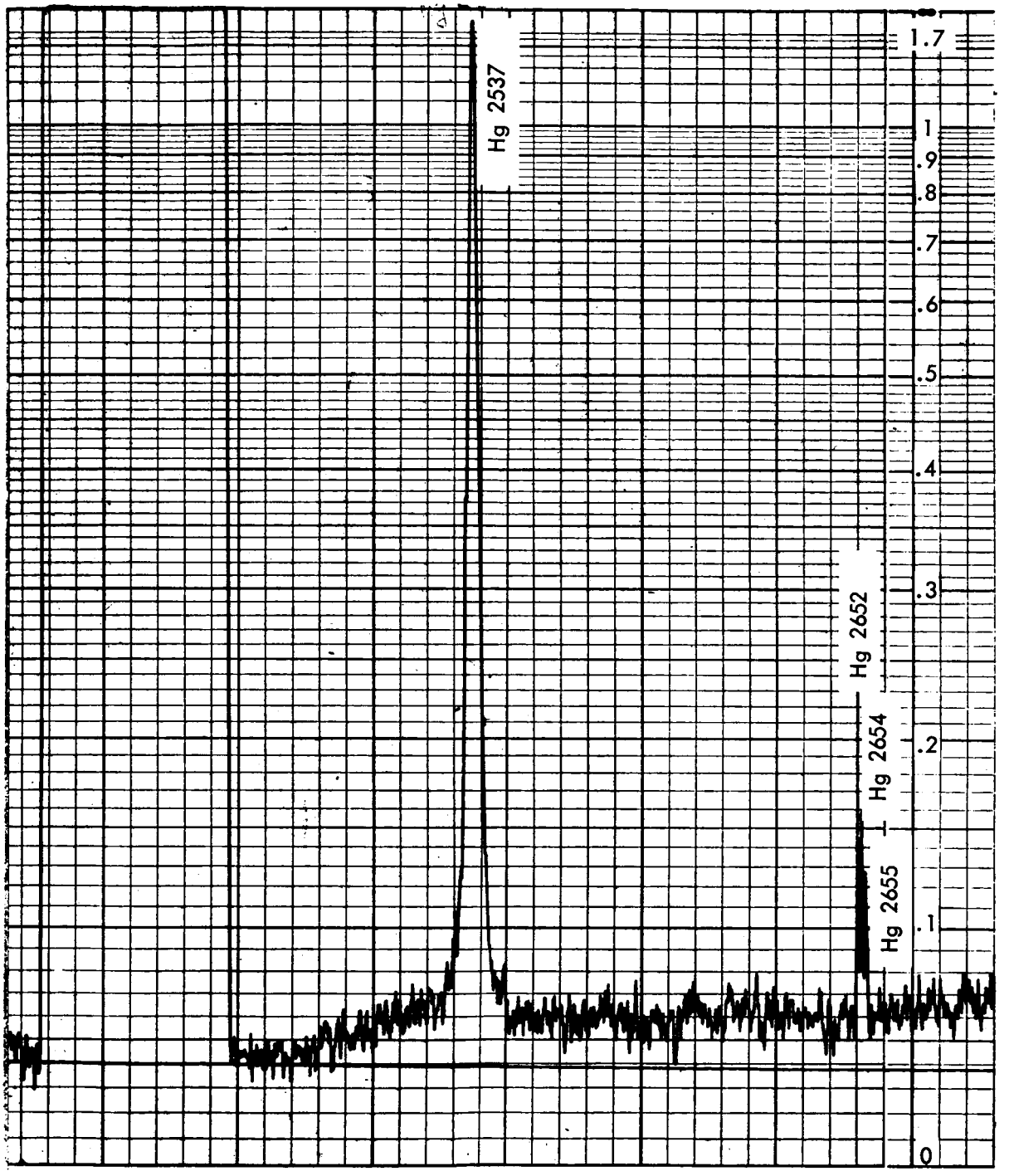

FIG. 15(a) DENSITOMETER TRACINGS OF THE 10/90 H_2/He MIXTURE RATIO SPECTROGRAM

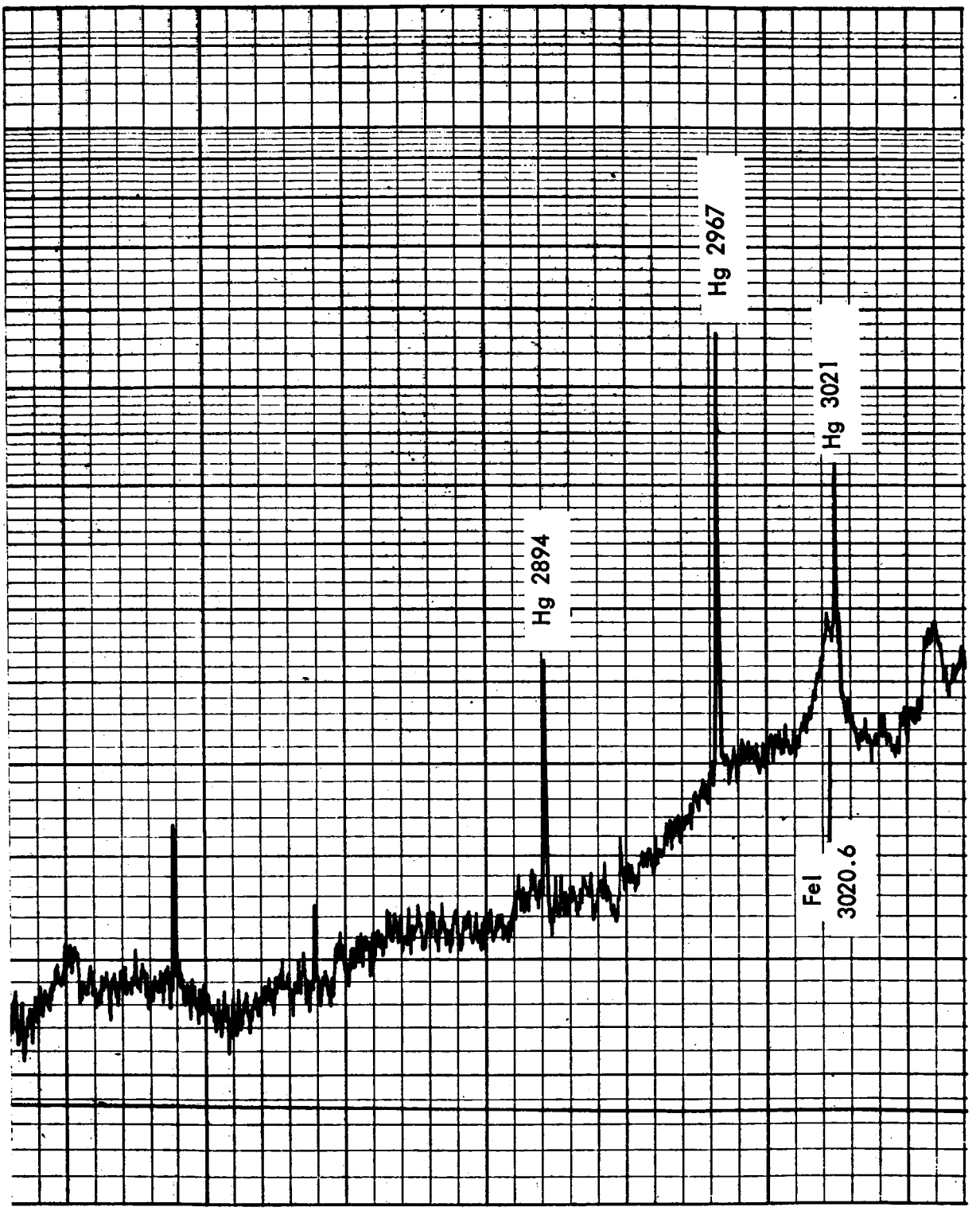

FIG. 15(b) DENSITOMETER TRACINGS OF THE 10/90 H_2/He MIXTURE RATIO SPECTROGRAM

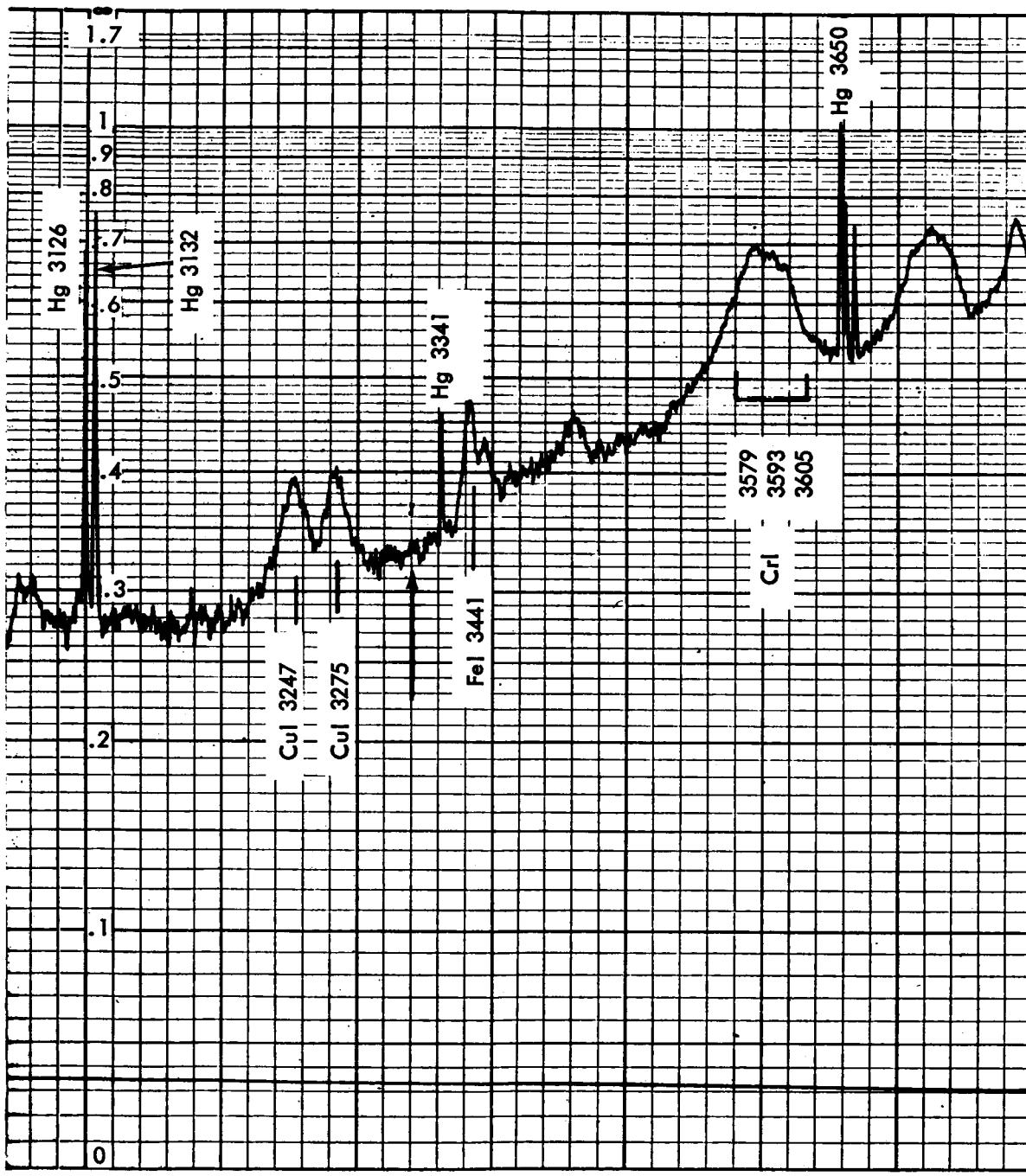

FIG. 15(c) DENSITOMETER TRACINGS OF THE 10/90 H_2/He MIXTURE RATIO SPECTROGRAM

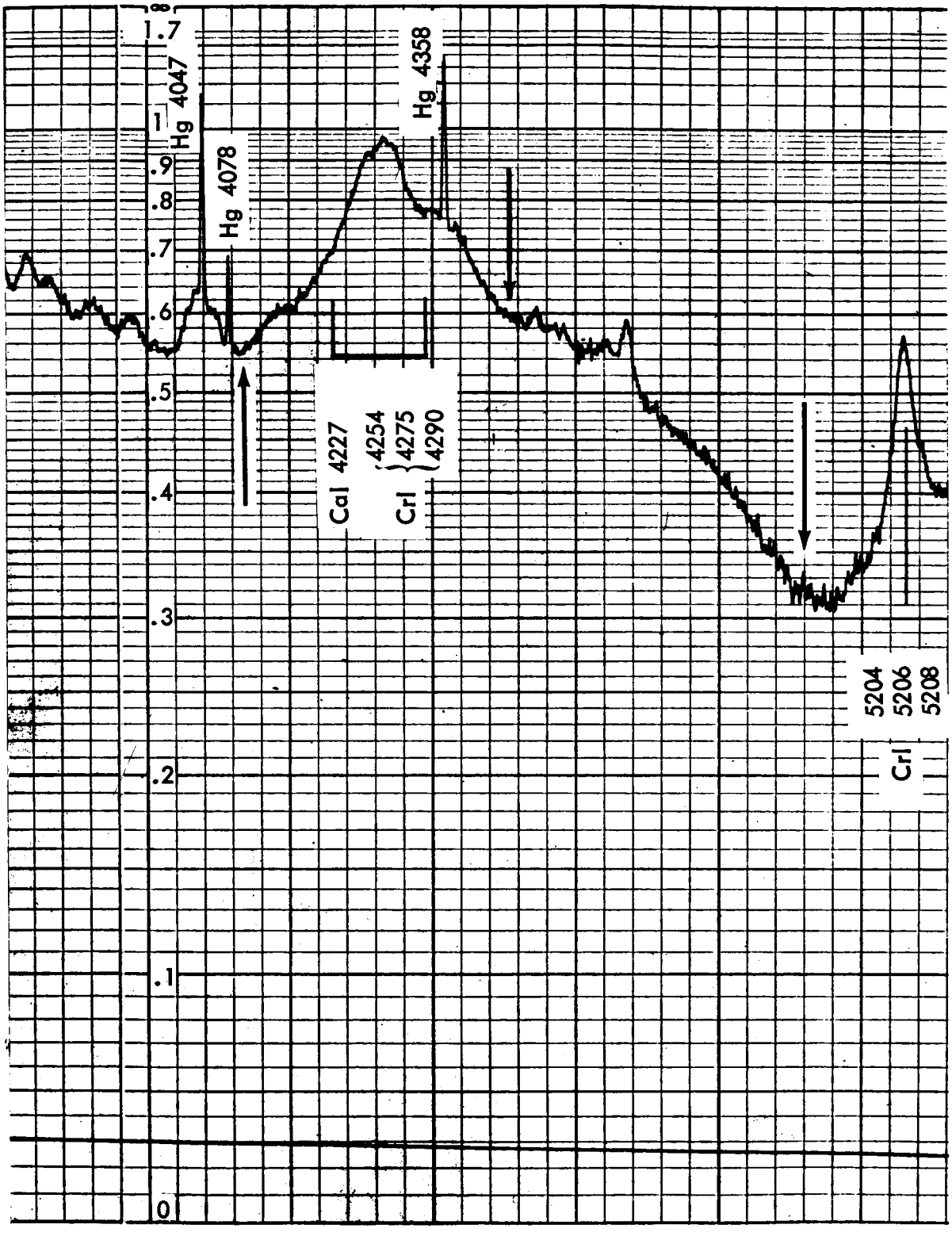

FIG. 15(d) DENSITOMETER TRACINGS OF THE 10/90 H_2/He MIXTURE RATIO SPECTROGRAM

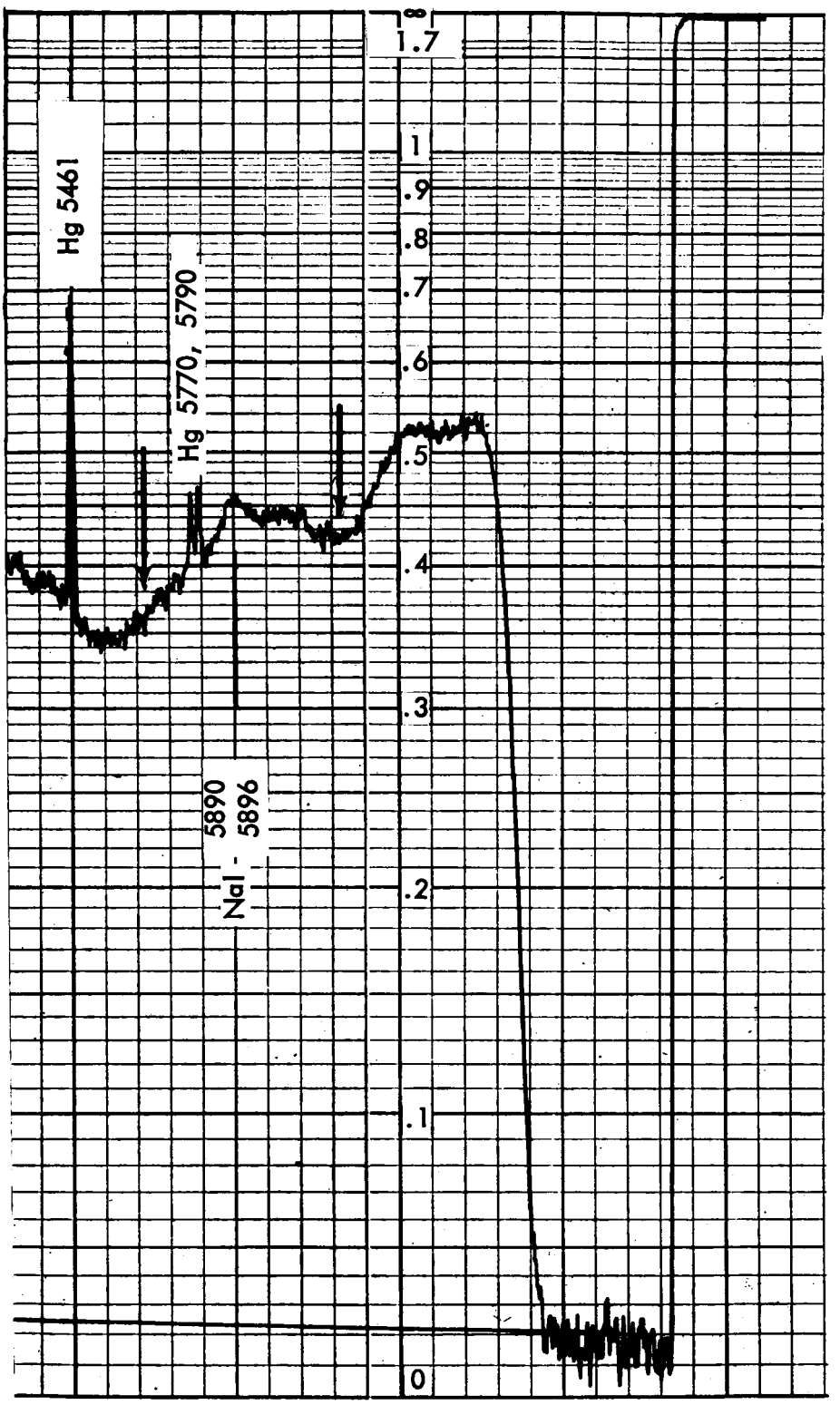

FIG. 15(e) DENSITOMETER TRACINGS OF THE 10/90 H_2/He MIXTURE RATIO SPECTROGRAM

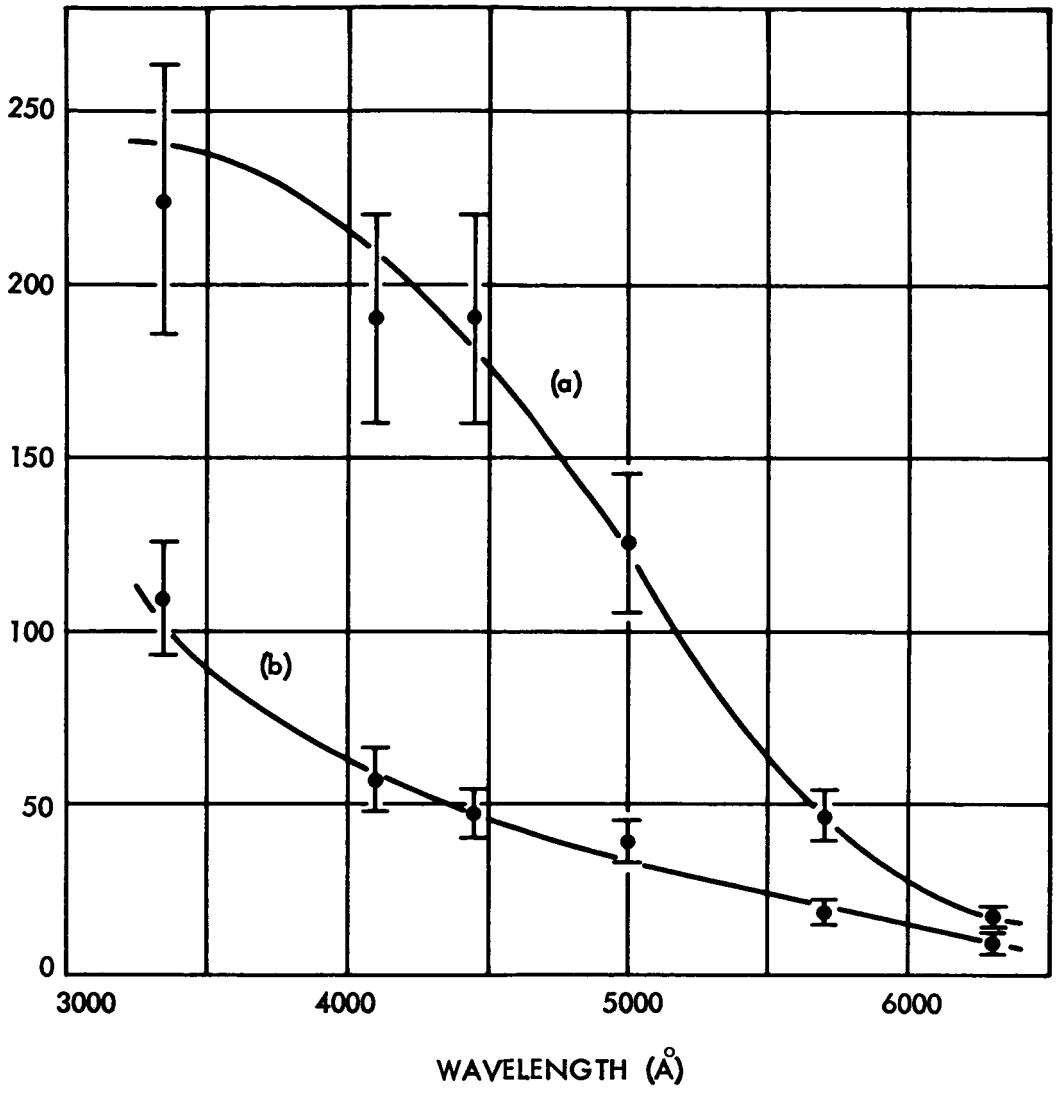

FIG. 16 CONTINUA INTENSITIES VS. WAVELENGTH
(a) PURE HELIUM AT 1830 ATM. AND 6040 °K
(b) 10/90 H_2/He AT 2630 ATM. AND 6160 °K.

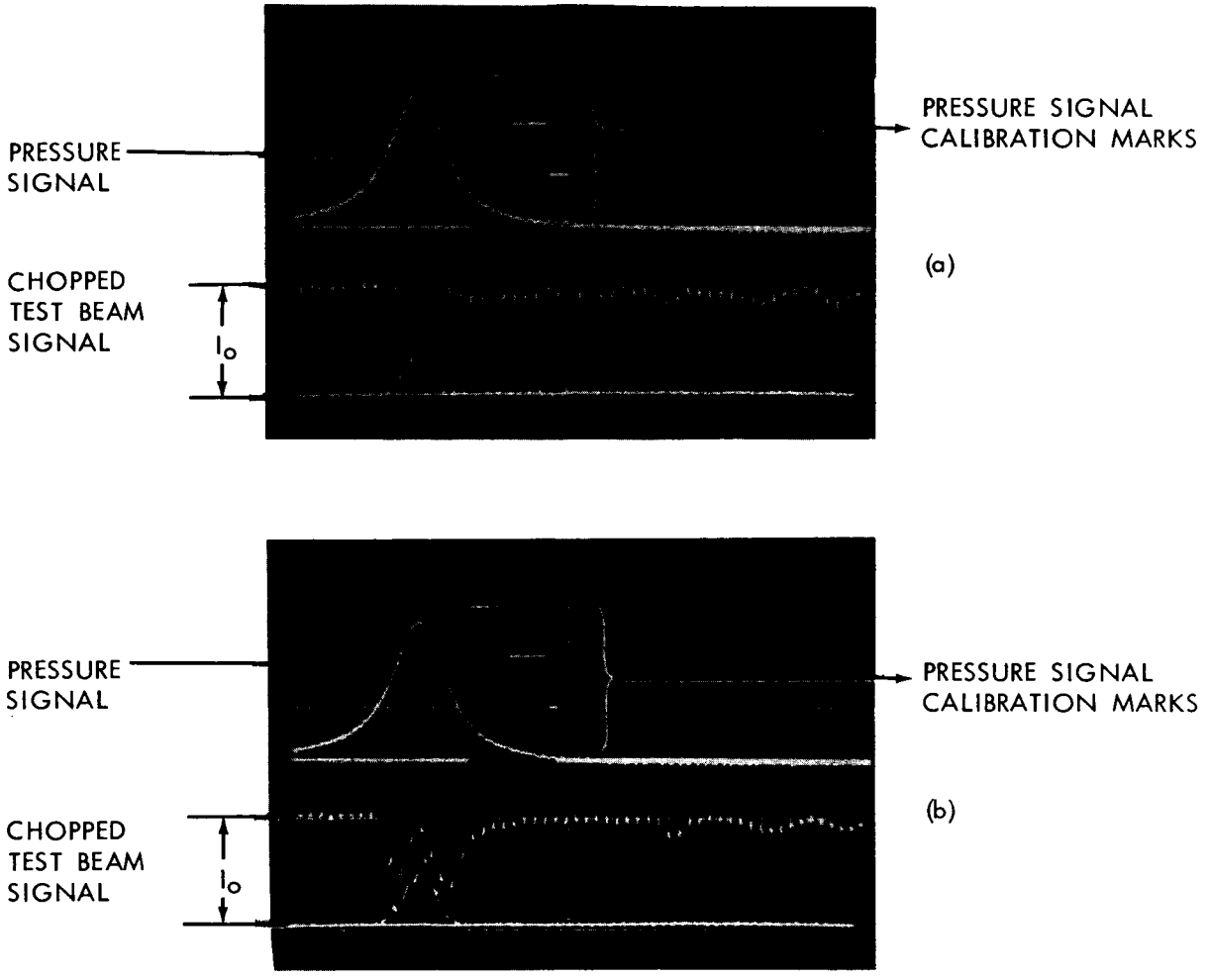

FIG. 17 OSCILLOSCOPE RECORDS FOR LINE OPACITY MEASUREMENTS
(a) CaI, λ 4227 Å, MAXIMUM PRESSURE = 750 ATM
(b) NaI, λ 5893 Å, MAXIMUM PRESSURE = 750 ATM
SWEEP SPEEDS = 2 MILLISEC/MAJOR DIVISION

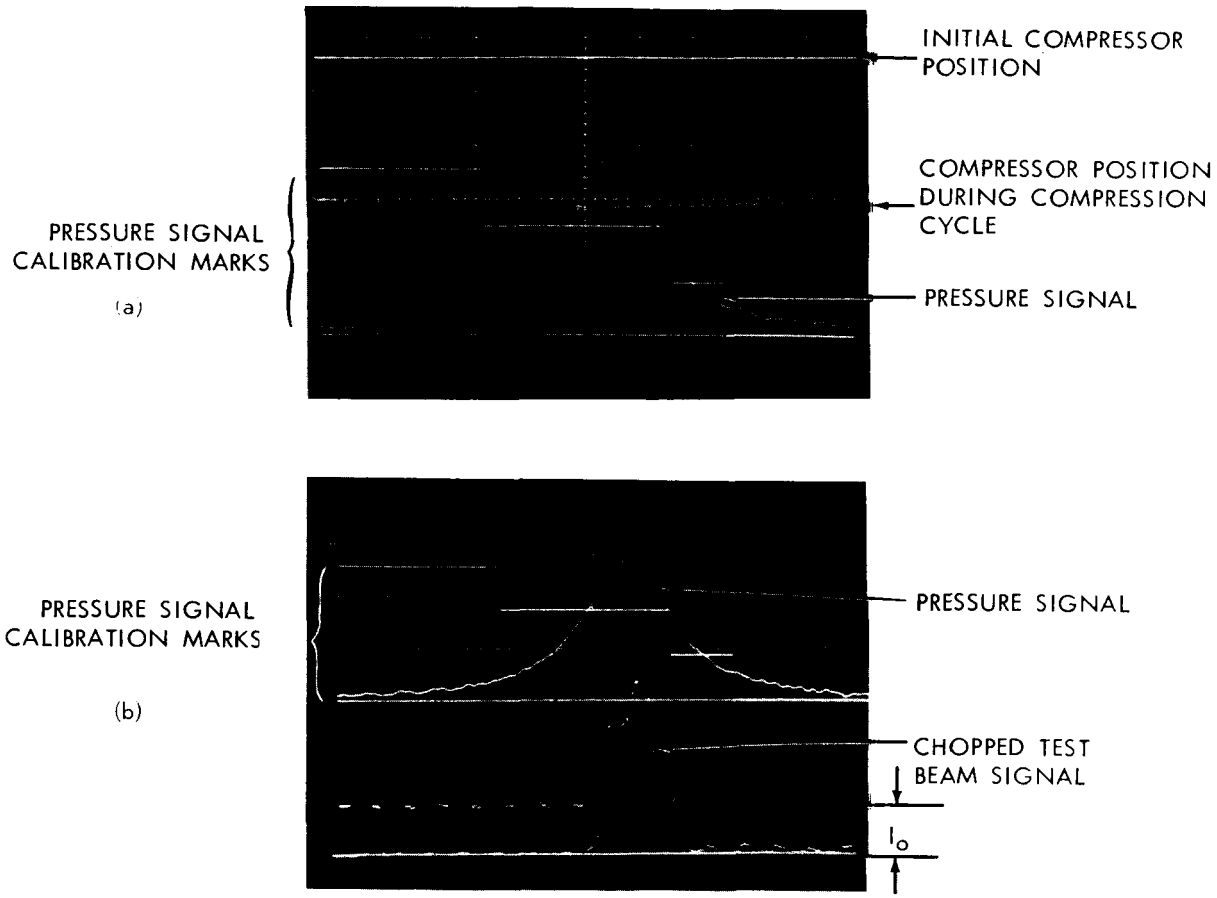

FIG. 18 OSCILLOSCOPE RECORDS FOR CONTINUUM OPACITY MEASUREMENTS
(a) PRESSURE AND MOTION RECORD
(b) PRESSURE AND TEST BEAM SIGNAL (5000 Å)
MAXIMUM PRESSURE = 1890 ATMOSPHERES
SWEEP SPEEDS = 500 μSEC/MAJOR DIVISION